**Title**
Fibrillin-1: Role in Integrin Mediated Cell Adhesion and Fibrotic Disease Progression



**Author**
Del Cid, Joselyn S

**Publication Date**
2018

Peer reviewed|Thesis/dissertation

# Fibrillin-1: Role in Integrin Mediated Cell Adhesion and Fibrotic Disease Progression

by

Joselyn Sarai Del Cid

DISSERTATION

Submitted in partial satisfaction of the requirements for the degree of

DOCTOR OF PHILOSOPHY

in

Cell Biology

in the

GRADUATE DIVISION

**Acknowledgements:**

We would like to thank Amha Atakilit for antibody purification from hybridoma banks and development of Sheppard lab blocking antibodies as well as Aparna B Sundaram for advice and suggestions on this work. We would also like to thank Kieu-My Huynh and Xiaozhu Huang for help developing the *in-vivo* mouse model measurements and subsequent data analysis. Additionally, we would like to thank Penny Handford and Sacha Jensen for sharing the DNA plasmid of the protein fragment utilized to complete this work and we would also like to thank Will DeGrado, Bobo Dang and Kathleen Molnar for help completing MS/MS profiling.

Fibrillin-1: Role in Integrin Mediated Cell Adhesion and Fibrotic Disease Progression

Joselyn Sarai Del Cid

**Abstract**

Fibrillins, large, multi-domain glycoproteins, are central organizers of elastin-containing microfibrils. They serve as scaffolds for the assembly of multi-protein complexes that contribute to the maintenance of tissue homeostasis and the regulation of growth factor signaling in the extracellular space. Fibrillin-1 is a modular glycoprotein that includes 7 latent transforming growth factor beta (TGFβ) binding protein-like (TB) domains and mediates cell adhesion through integrin binding to an exposed arginine, glycine, aspartic acid (RGD) motif in its 4th TB domain. A subset of missense mutations within TB4 cause Stiff Skin Syndrome (SSS), a rare autosomal dominant form of scleroderma. The fibrotic phenotype of this disease is thought to be regulated by changes in the ability of fibrillin-1 to mediate integrin binding. We characterized the ability of each RGD-binding integrin to mediate cell adhesion to fibrillin-1 or the SSS disease-causing variant. Our data show that 7 of the 8 RGD-binding integrins can mediate adhesion to fibrillin-1, four of which had not been previously described (αvβ5, αvβ1, α8β1 and αIIbβ3). A single amino acid substitution responsible for SSS (W1570C) markedly inhibited adhesion mediated by integrins α5β1, αvβ5, and αvβ6, partially inhibited adhesion mediated by αvβ1 and did not inhibit adhesion mediated by αvβ3, α8β1 or αIIbβ3. In the SSS mutant background, introduction of a new cysteine residue in place of a highly conserved tryptophan-1570 places a free sulfhydryl within range of three disulfide bonds. Introduction of this free sulfhydryl did not cause the protein to dimerize but instead induced a subtle change in the conformation of the RGD site that specifically, and differentially, mitigated interaction with only a subset of fibrillin-1-binding integrins. The goal of this work was to determine the relationship between fibrillin-1 and the RGD-binding integrins. Understanding how the mutation changes the dynamics of integrin binding could highlight a mechanism for future development of therapeutics in scleroderma.

**Table of Contents**

**List of Tables**

**List of Figures**

Chapter One

# Introduction

## Fibrillin-1 and the Extracellular Matrix

Fibrillins, large, multi-domain glycoproteins, are central organizers of elastin-containing microfibrils and serve as scaffolds for the assembly of multi-protein complexes that contribute to the maintenance of tissue homeostasis and the regulation of growth factor signaling in the extracellular space (1). Three different variants of fibrillin are present in humans; fibrillin-1 (FBN1), fibrillin-2 (FBN2) and fibrillin-3 (FBN3) (2). All three variants are ~350 kDa proteins that are structurally related to the latent TGFβ-binding proteins (LTBPs). Fibrillin-1 is the major component of tensile-strength transmitting microfibrils in the extracellular matrix (ECM) and self-assembles into 10-12 nm diameter filamentous microfibrils that provide the structural template for deposition of elastin fibers (3,4). In invertebrate species and in the elastin-free tissues of vertebrates, it is the fibrillin-1 containing microfibrils that confer the properties of elasticity and extensibility to the ECM (3). Mutations in FBN1 cause the connective tissue disorder, Marfan syndrome (MFS), and other related disorders (5-7). FBN2 has been shown to play a more primary role in the formation of microfibrils during embryonic development, and mutations in this variant lead to congenital contractural arachnodactyly (8). Much less is known about FBN3; like FBN2, its expression pattern is highest in fetal tissues and it localizes predominately to the brain (9).

The genomic organization of fibrillin-1 was originally described by Pereira et al in 1993 (10). Fibrillin-1 was shown to be structurally composed of 5 distinct domains (Fig 1). Like the LTBPs and many other extracellular and cell surface proteins, fibrillin-1 contains a large number of cysteine rich sequences that are homologous to epidermal growth factor (EGF). These EGF-like domains compose approximately 75% of the protein and of the 47 EGF-like domains, 43 are calcium binding (cbEGF) (11). Fibrillin-1 also contains 7 TGFβ binding protein-like domains (TB) that are similar to domains found in the LTBP family (12). The remaining domains exist at lower frequency; a fibrillin unique N-terminal (FUN) domain, a

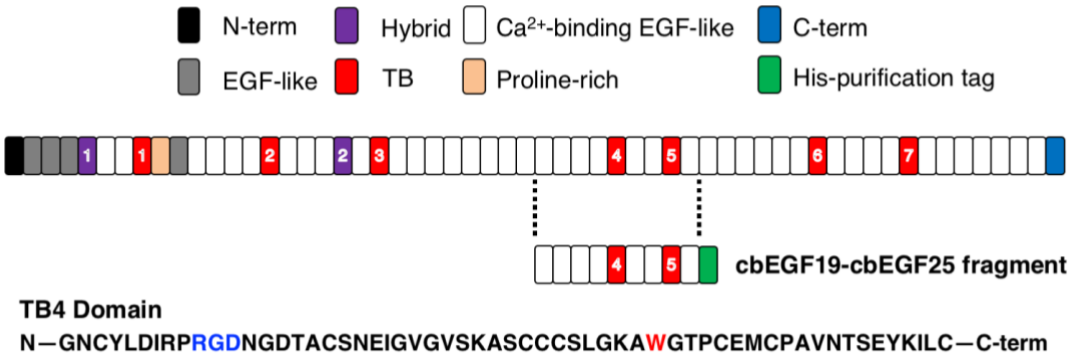


**Figure 1. Arrangement of Fibrillin-1 Domains:** The fibrillin-1 sequence is composed predominantly by 47 EGF-like domains, 43 which are $Ca^{2+}$ binding. The repeating structural domains of fibrillin-1 are defined at the top of the figure. The fragment cbEGF19-cbEGF25, containing the 4th TB repeat, was purified in a human mammalian system using the adjoining His-tag. The amino acid sequence for part of domain TB4 denotes the location of the RGD domain and the subsequent tryptophan that is mutated in the SSS background.

proline rich domain and 2 hybrid domains that share similarities with both the EGF-like and TB domains (13). While the precise organization of fibrillin within microfibrils remains unclear (though models have been proposed), specific segments of fibrillin-1 and 2 have been shown to interact *in vitro* with several extracellular and cell surface molecules, including fibronectin, fibulins, LTBPs, bone morphogenetic proteins (BMPs), syndecans and integrins (5). These multiple interactions are believed to drive the assembly of distinct macroaggregates in the ECM that impart the structural integrity of individual tissues and organs as well as localize TGFβ and BMP complexes within the ECM, thus controlling the signaling pathways and behavior of surrounding cells.

**Fibrillin in Health and Disease**

The majority of fibrillin-1 mutations have been linked to the development of MFS, a connective tissue disorder that is characterized by defects in the skeletal, cardiovascular and ocular systems (6,7). Deficiencies in the cardiovascular system, particularly development of aortic root dilation, are the main cause of mortality and morbidity in patients with MFS (14). Mutations in the human fibrillin-1 gene (FBN1) are particularly interesting because they are associated with a wide spectrum of clinical severity in MFS, irrespective of where they are located in the protein or how much they reduce gene expression.

Alternatively, there is strict correlation between a subset of missense mutations within a single domain, TB4, and the development of stiff skin syndrome (SSS), a vastly phenotypically dissimilar disease characterized by short stature, joint stiffness and thickening of the skin (5,15).

SSS is a rare but autosomal dominant form of scleroderma that was initially described in 1971 (15). Patients with SSS show altered deposition of fibrillin-1, elastin and collagen that results in the disruption of cell-matrix interactions. The dermis of SSS patients is packed tightly with abnormally dense microfibrillar aggregates and collagen bundles. The abnormal colocalization of elastin and fibrillin-1 in SSS has been shown to result in accumulation of nuclear phosphorylated SMAD2 (pSMAD2) and expression of connective tissue growth factor (CTCF), both targets of TGFβ signaling. Furthermore, fibroblasts plated on an SSS mutated fibrillin-1 fragment show reduced amounts of phosphorylated focal adhesion kinase (pFAK), an event that is mediated by the interaction of RGD ligands with cell surface integrins. While there have only been ~40 documented cases of SSS, the specific mutations that result in this fibrotic phenotype were not identified until 2010 (16). Work completed by genotyping four families with SSS showed that only mutations in TB4 that result in either the addition or deletion of a single cysteine residue and lead to an odd number of cysteines results in the development of SSS.

Work published in 2013 by Gerber et al. described the development of two mouse models that recapitulated the skin stiffing and thickening of SSS by introducing the homologous human tryptophan to cysteine mutation at residue-1570 or by mutating the RGD sequence at residues 1543-1545 to RGE (D1545E) (17). Both mice showed an increased deposition of collagen and decrease in subcutaneous fat in the dermis. As seen in patients, they developed disorganized and excessive microfibrillar aggregates. The abnormal skin stiffness in these mice was inhibited by treatment with a blocking antibody to TGFβ, suggesting that excessive TGFβ activity might be the cause of the cutaneous abnormalities.

In most cells, TGFβ is secreted as a latent complex comprised of a dimer of mature TGFβ, a non-covalently associated dimer of an N-terminal fragment encoded by the same gene (called the latency-associated protein (LAP)), and a latent TGFβ binding protein (LTBP) (18-20). Select members of the

integrin family ($\alpha v\beta 1$, $\alpha v\beta 6$ and $\alpha v\beta 8$) play critical roles in the activation of the latent cytokine which requires integrin binding to an exposed RGD motif in LAP (21-25). Aberrant integrin-mediated activation of TGFβ can contribute to excessive deposition of extracellular matrix (ECM) and lead to the development of fibrosis.

**Fibrillin: Structural Insights**

The structural composition of fibrillin-1 has been shown to be heavily dependent on two factors, $Ca^{2+}$ ion concentration and strict pairing of an even number of cysteine residues that are all sequestered in disulfide bonds within the EGF, the hybrid and TB domains. The soluble structure of domains cb32-33 identified a rigid rod-like arrangement of the two domains that was stabilized by interdomain calcium binding and hydrophobic interactions (26). Loss of calcium binding has been shown to dramatically change the morphology of microfibrils, causing the rod-like lateral conformation to become diffuse and much less well defined. These structural elements of fibrillin-1 have been determined to play crucial roles in the progression of both MFS and SSS. Early studies into the structural arrangement of fibrillin-1 identified a subset of MFS-causing mutations that altered calcium binding consensus residues in several of the cbEGF domains (11).

In the absence of extensive secondary structure and an extended hydrophobic core, the individual domains of fibrillin-1 rely on a large number of disulfides for structural stability. In SSS specifically, the large hydrophobic residue (Trp-1570) plays a prominent role in packing against adjacent disulfide bonds, and hence in stabilizing their pairing. Since the eight-cysteine motif of TB4 is responsible for stabilizing the globular structure of this domain, the addition of a new cysteine residue at position 1570 has the potential to change the stability of the mutant fragment by causing the reshuffling of disulfide bonds. This hypothesis is further enhanced by genomic mapping of the fibrillin-1 mutations that cause SSS in humans; all result in the either the gain or loss of a cysteine residue.

**Integrin and Fibrillin-1 Interactions**

TB4 is the only domain in fibrillin-1 that contains an exposed arginine, glycine, aspartic acid tri-peptide (RGD), a common recognition motif for binding a subset of members of the integrin family (27). While a few integrins have been shown to interact with the local RGD site of TB4 (28-30), it is well known that different RGD-binding integrins preferentially interact with RGD sites depending on the surrounding sequences and on the secondary and tertiary structures of ECM proteins (31-32). The likely structural effects of an unpaired cysteine in the mutations known to cause SSS further highlights the possibility that perturbation of the interactions between fibrillin-1 and integrins could be mechanistically linked to SSS.

Integrins are transmembrane proteins that are composed of an α and β subunit. 18 α and 8 β subunits have been identified and they heterodimerize to form 24 different integrin partners. Within those 24, different subsets have been shown to preferentially bind specific ECM proteins, including the collagen and laminin integrin receptors (33-34). The RGD-binding subfamily is a subset of 8 integrins that mediate integrin binding to ligands that contain an exposed RGD motif. Within the RGD-binding subfamily, a subset of these have been shown to mediate TGFβ activation. This occurs through integrin binding to an RGD motif in LAP that results in the transmission of force from contracting cells and pulls apart the latent TGFβ complex thus releasing active cytokine. TGFβ is then free to interact with its own cell surface receptors and turn on downstream signaling pathways through phosphorylation of SMAD2/3 and SMAD independent pathways (20-21). The relationship between the RGD-binding integrins, the ECM and TGFβ activation has led to proposed mechanisms of disease progression, specifically within the context of fibrosis. Our lab and others have previously shown that 3 integrins, αvβ1, αvβ6 and αvβ8, can bind to the RGD site in TGFβ LAP and activate latent TGFβ (22-25). TGFβ activated by two of these, αvβ6 and αvβ1, has been shown to contribute to tissue fibrosis in the lung, liver and kidney. It was this relationship that led us to hypothesize that in SSS, loss of binding of one or more of these TGFβ activating integrins to fibrillin-1 could free these integrins up to bind and activate local TGFβ, which could contribute to skin fibrosis.

Prior reports have suggested that three integrins, αvβ3, α5β1 and αvβ6 can bind to the RGD domain of fibrillin-1. The binding capacities of integrins αvβ3 and α5β1 were determined through cell-based assays measuring adhesion to fibrillin-1 or through changes in cell spreading and cytoskeletal rearrangement (5, 28, 29). A more quantitative approach using surface plasmon resonance (SPR) analysis by Jovanovic et al in 2007, concluded that αvβ6 can also bind fibrillin and has a low $k_d$ value for fragments containing the TB4 domain (30, 35). However, among these three identified integrins, only αvβ6 has been definitively shown to mediate activation of TGFβ. There are 8 well-characterized RGD-binding integrins; αvβ1, αvβ3, αvβ5, αvβ6, αvβ8, α5β1, α8β1 and αIIbβ3 (36). The relative effectiveness of each of these integrins to bind fibrillin-1, and the effects of the disease-causing mutations on interactions with the full range of RGD-binding integrins has not been systematically evaluated.

This work sought to more thoroughly examine the interactions between fibrillin-1, the RGD-binding integrin subfamily and TGFβ activation. We developed cell-based assays to systematically study the ability of each of the RGD-binding integrins to mediate cell adhesion to fibrillin-1. We further sought to determine how the most common SSS missense mutation in the TB4 domain might differentially affect binding to each fibrillin-binding integrin. We found that 7 of the 8 RGD-binding integrins can mediate adhesion to fibrillin 1, but that adhesion mediated by only 4 of these (αvβ1, αvβ5, αvβ6, and α5β1) is affected by the SSS mutation. Our findings thus identify a subset of RGD-binding integrins through which inhibition of binding to mutant fibrillin could contribute to the development of SSS.

Chapter Two

# The SSS mutation in fibrillin-1 differentially regulates integrin binding

## Purification of fibrillin-1 fragments from mammalian cells

To determine which members of the RGD-binding integrin subfamily recognize the RGD sequence in fibrillin-1, human recombinant fragments containing domains cbEGF19-cbEGF25, which included TB4 containing the RGD motif, were purified from HEK293FS cells (Fig 1). Fragments were purified for the wildtype protein, the SSS disease-causing mutant and a loss-of-integrin binding control mutant.

## Characterization of cell-based systems

We utilized cell adhesion assays to systematically evaluate the ability of the 8 known integrins that bind to RGD-containing ligands to bind to fibrillin-1. For 6 of these, $\alpha5\beta1$, $\alpha8\beta1$, $\alpha v\beta3$, $\alpha v\beta5$, $\alpha v\beta6$, and $\alpha v\beta8$, we used SW480 cells, a colon cancer cell line that endogenously expresses $\alpha v\beta5$ and $\alpha5\beta1$ but does not express any of the remaining RGD-binding integrins (Fig 2A, C). We used transfected SW480 cells expressing individual integrin subunits, $\beta8$, $\beta3$, $\beta6$ or $\alpha8$, as previously described (22-24), to induce high cell surface expression levels of $\alpha8\beta1$, $\alpha v\beta3$, $\alpha v\beta6$ and $\alpha v\beta8$, respectively (Figure 2B). SW480 cells cannot be induced to express functional $\alpha v\beta1$ or $\alpha IIb\beta3$. Integrin $\alpha v\beta1$ was therefore evaluated using human dermal fibroblasts (HDF), which endogenously express functional $\alpha v\beta1$ (Fig 2E). They also express integrins, $\alpha v\beta3$, $\alpha v\beta5$ and $\alpha5\beta1$ (Fig 2D). Integrin $\alpha IIb\beta3$ has been shown to be expressed on the cell surface of platelets and was evaluated using human platelets freshly isolated from whole blood (37).

## 7 of the 8 RGD integrins mediate cell adhesion to wild-type fibrillin-1

To assess the potency of each integrin to individually mediate adhesion to wild-type fibrillin-1, we isolated the effects of each integrin by blocking every other RGD binding integrin expressed by the utilized cell type and quantified adhesion to dishes coated with a wide range of fragment concentrations. Thus, for

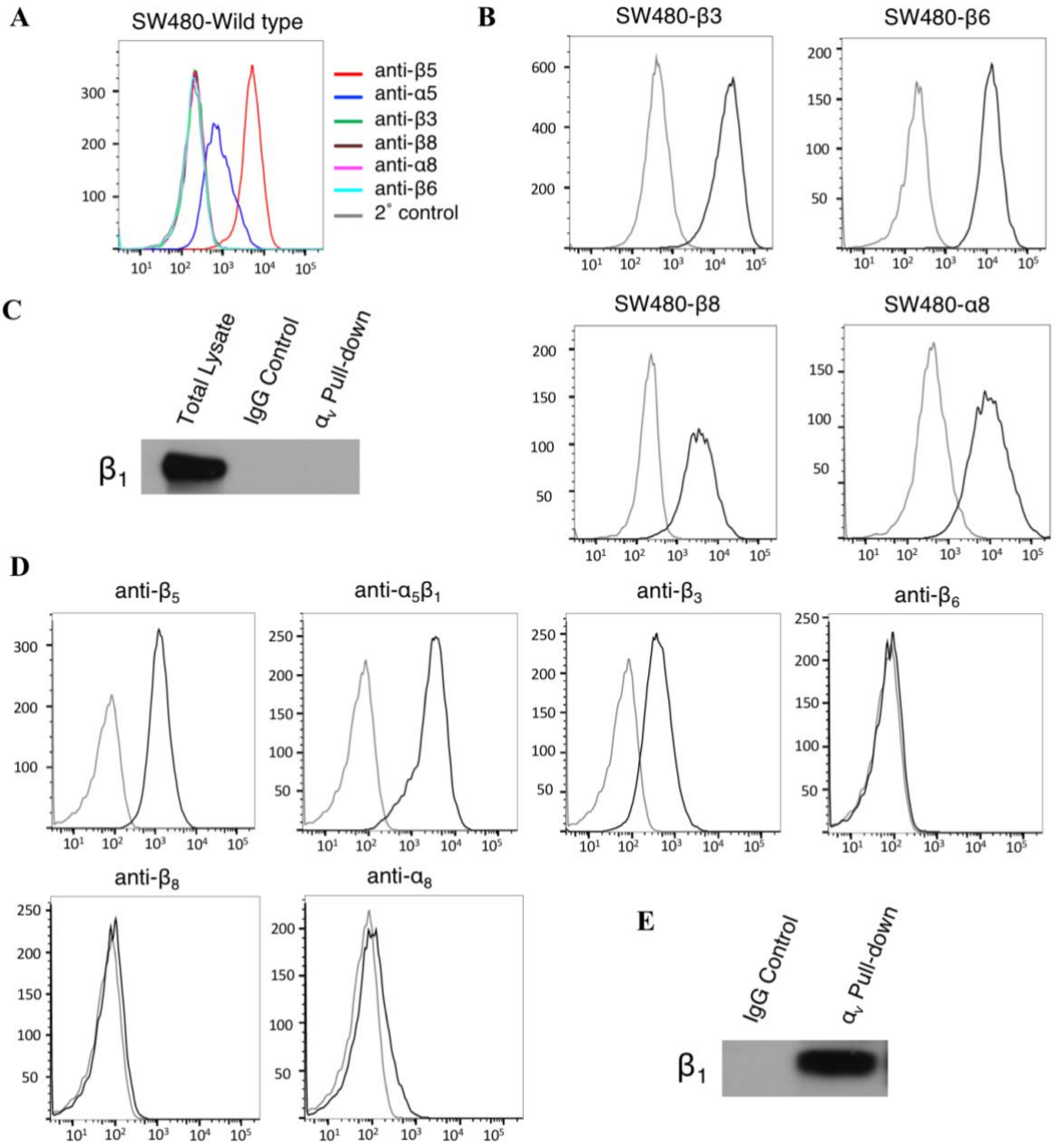


**Fig 2. Integrin Profile of Cell System:** **(A)** SW480 cells show high surface expression of both endogenous and **(B)** transfected integrin subunits. Cells were labeled in suspension with primary antibodies against specific cell surface integrins followed by incubation with a secondary antibody conjugated to phycoerythrin (PE). Cells were analyzed by flow cytometry and gated for live cells. Representative histograms of PE expression versus cell count are shown, x-axis: PE expression (mean fluorescence intensity), y-axis: cell count. **(C)** Cell surface expression of αvβ1 was measured by IP-WB. SW480 cells were lysed in RIPA buffer and incubated with a primary antibody against αv. Sepharose G beads were used to pulldown primary antibody, resulting solution run on 8% SDS-PAGE and western-blotted for β1 expression. **(D)** HDF show varying levels of cell surface expression of the RGD-binding integrin family. **(E)** Cell surface expression of αvβ1 in HDF was measured by IP-WB as described above.

wild-type SW480 cells, adhesion mediated by α5β1 was determined in the presence of blocking antibody to αvβ5 (ALULA) and adhesion mediated by αvβ5 was determined in the presence of blocking antibody to α5β1 (P1D6). For SW480 cells transfected to express additional integrins, adhesion mediated by the heterologously expressed integrin was assessed in the presence of blocking antibodies to both α5β1 and αvβ5 (Table 1).

In each panel we compare data for adhesion of the cell line used in the absence of any blocking antibody to adhesion in the presence of blocking antibodies against all other expressed RGD-binding integrins (Figure 3). We found that αvβ5 and αvβ3 were both highly effective receptors for wild-type fibrillin-1 (Fig 3A, B). α5β1 and α8β1 also mediated adhesion, but to a lesser degree (Fig 3C, D). However, the comparatively weak binding mediated by α5β1 could be explained by the relatively low expression of α5β1 in wild-type SW480 cells. αvβ6 only weakly mediated adhesion, and αvβ8 did not mediate adhesion at all (Fig 3E, F).

As noted previously, evaluations of integrins αvβ1 and αIIbβ3 were completed using cell adhesion assays with HDF and human platelets, respectively. Individual contribution of αvβ1 was completed using HDF in the presence of blocking antibodies against αvβ3 (AXUM2), αvβ5 and α5β1. The contribution of αIIbβ3 was evaluated using human platelets in the presence of pan-specific αv and β1-blocking antibodies.

**Table 1.** *Antibody Blockade for Integrin Isolation in Cell Adhesion Assays*

| Integrin | Cell Line | Antibodies for Integrin Isolation | Antibodies for Complete Blockade |
|---|---|---|---|
| α5β1 | SW480 | ALULA | ALULA + P1D6 |
| αvβ5 | SW480 | P1D6 | ALULA + P1D6 |
| αvβ3 | SW480-β3 | ALULA + P1D6 | ALULA + P1D6 + AXUM2 |
| αvβ6 | SW480-β6 | ALULA + P1D6 | ALULA + P1D6 + 3G9 |
| α8β1 | SW480-α8 | ALULA + P1D6 | ALULA + P1D6 + YZ83 |
| αvβ8 | SW480-β8 | ALULA + P1D6 | ALULA + P1D6 + ADWA-11 |
| αvβ1 | HDF | ALULA + P1D6 + AXUM2 | L230 + P5D2 |
| αIIbβ3 | Human platelets | L230 + P5D2 | L230 + P5D2 + 10E5 |

Cells were exposed to combination antibody treatments for isolation of specific integrin mediated adhesion. All antibodies were added at 10 μg/mL to cells suspended in FBS-free medium and incubated on ice for 10 min before plating on fibrillin-1 coated plates.

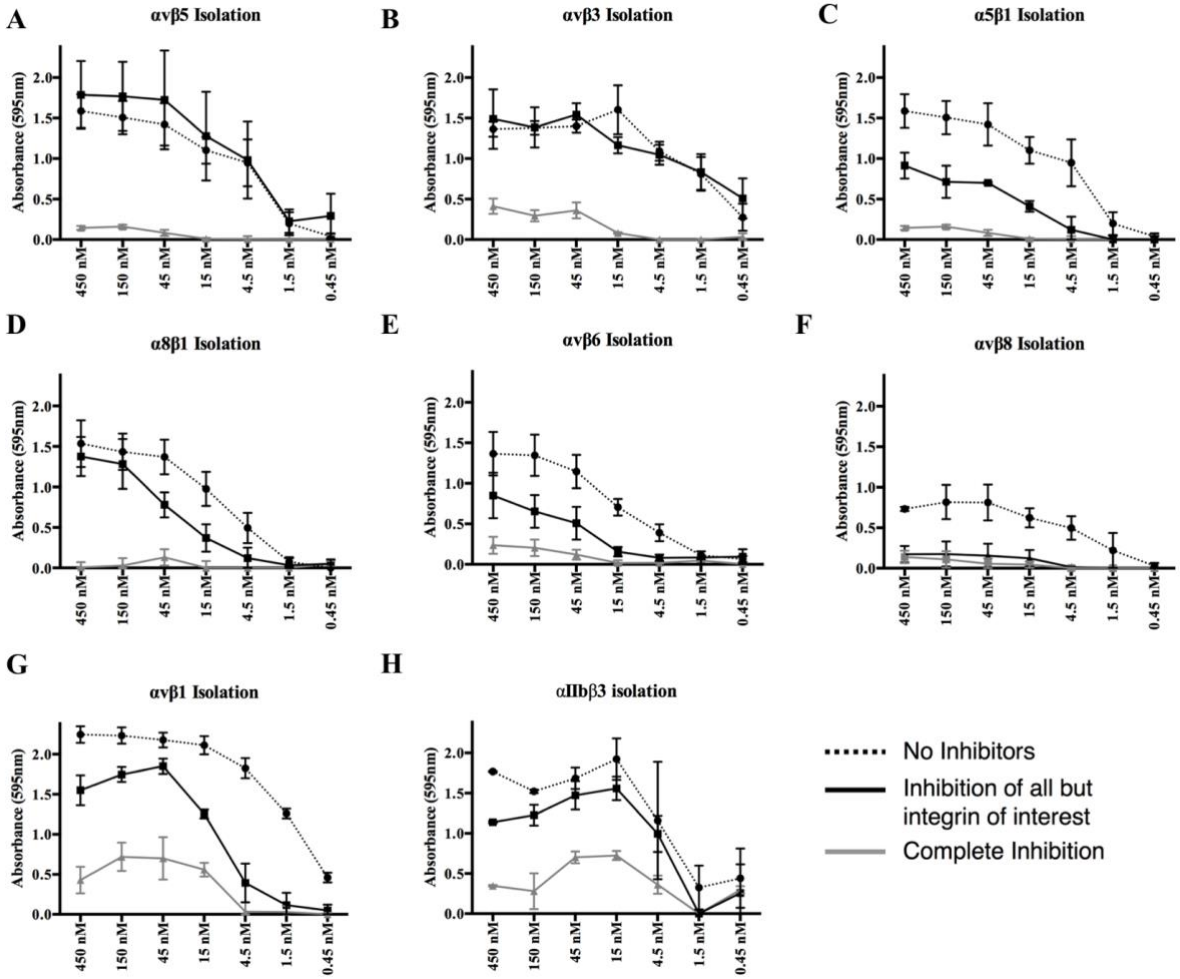


**Figure 3. Isolation of the RGD-binding Integrins to Wild-type Fibrillin-1:** Binding capacities of the RGD-integrin family to wild-type fibrillin-1. **(A)** Cell adhesion of integrin αvβ5 in SW480 cells, completed in the presence of P1D6. **(B)** Cell adhesion of integrin αvβ3 in SW480 cells transfected with integrin β3, completed in the presence of P1D6 and ALULA. **(C)** Cell adhesion of integrin α5β1 in SW480 cells, completed in the presence of ALULA. **(D)** Cell adhesion of integrin α8β1 in SW480 cells transfected with integrin α8, completed in the presence of P1D6 and ALULA. **(E)** Cell adhesion of integrin αvβ6 in SW480 cells transfected with integrin β6, completed in the presence of P1D6 and ALULA. **(F)** Cell adhesion of integrin αvβ8 in SW480 cells transfected integrin β8, completed in the presence of P1D6, ALULA and 3G9. **(G)** Cell adhesion of integrin αvβ1 in HDF, completed in the presence of P1D6, ALULA and AXUM2. **(H)** Cell adhesion of integrin αIIbβ3 in human platelets isolated from whole blood, completed in the presence of L230 and P5D2. Data represents mean of 3 replicates +/- SEM.

Both cell types bound well to wild-type fibrillin-1 in the absence of blocking antibodies. Isolation studies with blocking antibodies allowed us to demonstrate that αvβ1 and αIIbβ3 are also highly effective integrin receptors for fibrillin-1 (Fig 3G, H), bringing the total number of integrins that can mediate adhesion to

fibrillin-1 to 7. We confirmed that the addition of blocking antibodies specific to the isolated integrin markedly reduced adhesion in every case, demonstrating the specificity of this assay system.

**The SSS Disease-Causing Mutation Differentially Regulates Integrin Binding**

We next determined how the SSS disease causing substitution (W1570C) affected adhesion mediated by each of the 7 integrins identified above. As shown in Figure 4, the disease-causing WC mutation virtually abolished adhesion mediated by αvβ5, α5β1 and αvβ6, but had no effect on adhesion mediated by αvβ3 or α8β1 (Fig 4A-E). In contrast, mutation of the RGD sequence to RGE dramatically inhibited binding of each of these 5 fibrillin-binding integrins. The SSS (WC) mutation substantially inhibited binding of αvβ1 to fibrillin-1, but this inhibition was not complete, with adhesion mediated to the WC mutant at an intermediate level between wild-type fibrillin-1 and the RGE mutant (Fig 4F). In contrast, the WC substitution did not inhibit binding mediated by integrin αIIbβ3. Rather, αIIbβ3-mediated adhesion was modestly increased by the WC mutation. As expected, the RGE mutation did substantially (albeit incompletely) inhibit αIIbβ3-mediated adhesion (Fig 4G).

Taken together, these results suggest that the effects on integrin-binding of the disease-causing WC mutation in fibrillin-1 are not uniform across integrin heterodimers. We demonstrated that 7 of the 8 RGD binding integrins can mediate cell adhesion to wild-type fibrillin-1. Four of these, α8β1, αvβ1, αvβ5 and αIIbβ3 have not been previously described as receptors for fibrillin-1. Mutation of the RGD sequence in the fourth TB domain to RGE, abrogated adhesion mediated by 6 of these integrins (α5β1, α8β1, αvβ1, αvβ3, αvβ5 and αvβ6) and substantially inhibited adhesion mediated by αIIbβ3, confirming that cell adhesion was mediated by direct interaction of each of these integrins with the RGD site in fibrillin-1. In contrast to the RGE mutation, the tryptophan to cysteine missense mutation responsible for causing SSS differentially affected binding of these integrins to fibrillin-1. Adhesion mediated by α5β1, αvβ5 and αvβ6, at the levels expressed on the respective cell lines, was entirely abrogated by the disease-causing mutation

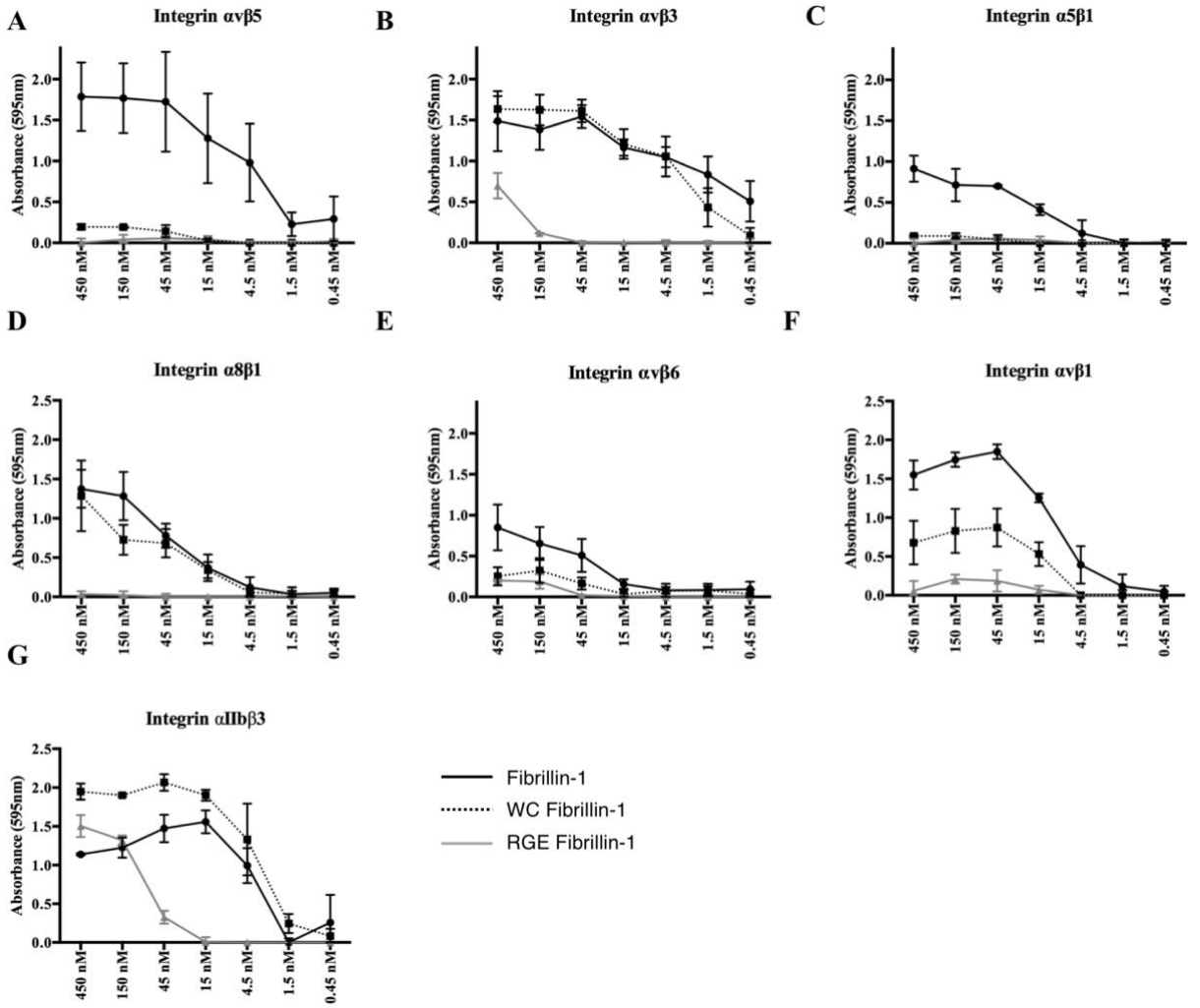


**Figure 4. WC Fibrillin-1 Differentially Regulates Integrin Binding:** Binding capacities of the RGD-integrin family to the wild-type, disease causing (WC) and RGE knock-out fragments. **(A-E)** Cell adhesion of endogenous and transfected integrins in SW480 cells. All conditions completed in the presence of blocking antibodies against all integrins but one of interest. **(F)** Cell adhesion of integrin αvβ1 in HDF, completed in the presence of P1D6, ALULA and AXUM2. **(H)** Cell adhesion of integrin αIIbβ3 in human platelets isolated from whole blood, completed in the presence of L230 and P5D2. Data represents mean of 3 replicates +/- SEM.

and adhesion mediated by αvβ1 was partially abrogated. In contrast, adhesion mediated by α8β1, αvβ3 and αIIbβ3 was either unaffected or modestly enhanced (in the case of αIIbβ3).

As noted in the introduction, mice expressing either a knock-in of a cysteine for tryptophan substitution in mouse fibrillin-1, at the same location as the human disease-causing WC mutation, and

knock-in of a glutamic acid for aspartic acid substitution in the exposed RGD site (RGE), both cause skin thickening reminiscent of stiff skin syndrome (14). Our cell adhesion assay results strongly support the hypothesis that SSS is due, at least in part, to loss of integrin binding to mutant fibrillin-1. Our results further suggest that the relevant integrin(s) would likely be $\alpha5\beta1$, $\alpha v\beta1$, $\alpha v\beta5$ or $\alpha v\beta6$, since the interaction between $\alpha8\beta1$, $\alpha v\beta3$ and $\alpha IIb\beta3$, the other 3 fibrillin-1 binding integrins, are not inhibited by the WC mutation but are markedly inhibited by substitution of glutamic acid for aspartic acid in the integrin-binding RGD site.

Chapter Three

## The SSS mutation alters the tertiary structure of fibillin-1

### *SSS fibrillin-1 mutant contains a free sulfhydryl*

The TB4 domain of fibrillin-1 is characterized by an eight-cysteine motif that forms four disulfide bridges responsible for stabilizing the protein fold (Fig 5A). The hydrophobic core of this domain is further stabilized by the presence of tryptophan at position 1570, a feature that is conserved in all TB domains in fibrillins and LTBPs. In the SSS mutant this conserved tryptophan, which in the wild-type structure is within range of three disulfide bonds (Fig 5B), is replaced with a cysteine. In the wild-type structure, the Cβ atom of the Trp-1570 residue is within 5 Å of both Cys-1534 and Cys-1562. This is within the Cβ-Cβ distance seen in disulfide bonds in proteins (38).

To determine if the free sulfhydryl remained free or induced dimerization of the mutant fragment, we measured the concentration of protein sulfhydryls using the Ellman's protocol. The Ellman's reagent was replaced with 4,4'-dithiodipyridine (DTDP), an alternative reagent whose small size and amphiphilic nature allow it to react quickly with poorly accessible residues (39). DTDP was reacted with the wildtype and mutant fragment of fibrillin-1 at a range of protein concentrations, from which a concentration of SH was determined. The slope of the resulting plot denotes the number of free sulfhydryls within a protein fragment. The low value of wild-type fibrillin-1 confirms that all the cysteine residues in the protein fragment are sequestered in disulfide bonds (Fig 5C). The SSS mutant, however, showed an increased slope close to the value of 1, suggesting that the mutant maintains a single free sulfhydryl without forming protein dimers. We further confirmed this observation by labeling the two proteins fragments with Alexa-Fluor™ 647 $C_2$ maleimide, a fluorescent dye that reacts specifically with thiol groups (Fig 5D) and by Coomassie staining the fragments in reduced versus non-reduced conditions (Fig 5E). Reaction of the mutant fibrillin-1 fragment with the fluorescent dye confirmed the presence of an additional free cysteine residue while the Coomassie staining demonstrated that both fragments remain monomers in solution.

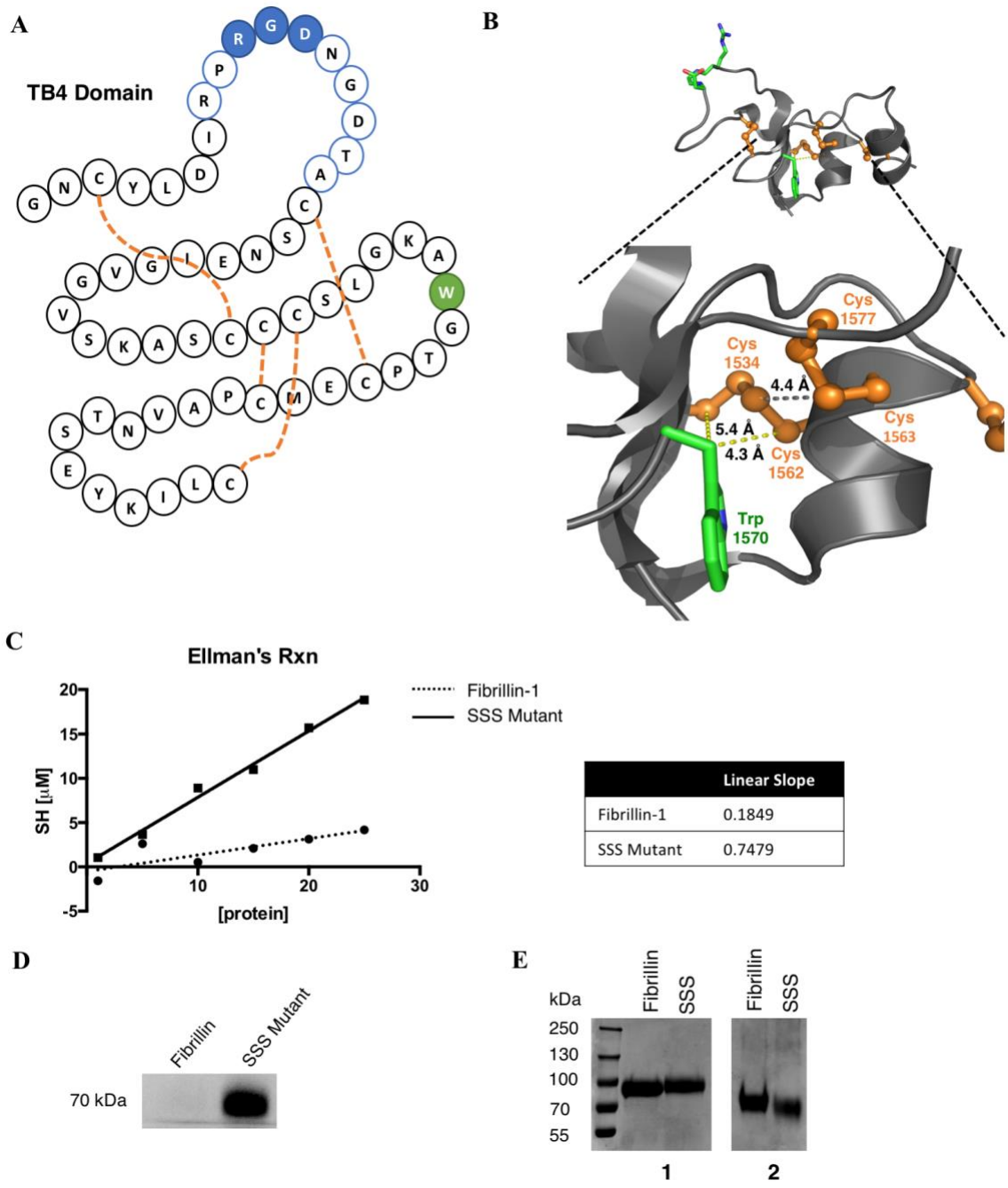


**Figure 5. WC Fibrillin-1 Contains a Free Sulfhydryl: (A)** Schematic of the TB4 domain in fibrillin-1. The flexible RGD loop is denoted in blue, tryptophan-1570 in green and the disulfide bridges by dashed orange lines. **(B)** Tertiary structure of TB4 from crystalized fragment (17). Amino acid 1570 shown in wild-type construct as tryptophan (green) and surrounding cysteines in orange. **(C)** Ellman's reaction completed using 4,4'-dithiodipyridine reagent on a serial dilution of wild-type and mutant fibrillin-1. Absorbance measurements were done in 1 cm cuvettes. **(D)** Fluorescent labeling of wild-type and mutant fibrillin-1 fragments using Alexa-Fluor™ 647 $C_2$ maleimide, labeled protein run on a 4-10% SDS-PAGE and imaged using the 650 nm laser line. **(E)** Coomassie staining of reduced (1) versus non-reduced (2) samples run on an 8% SDS-PAGE.

The cell adhesion data strongly suggest that the SSS mutation does not simply eliminate integrin interactions with the RGD sequence in the TB4 domain. Introduction of a free sulfhydryl does not cause the protein to dimerize but instead induces a subtle change in the conformation of the RGD site that specifically, and differentially, mitigates interaction with only a subset of fibrillin-1-binding integrins.

***The SSS mutant shows overall reduction in protein structure***

Confirmation of the free cysteine in the mutant fragment prompted us to consider the possibility that the addition of a new cysteine residue was reshuffling the formation of disulfide bridges within TB4. We attempted to answer this question through mass spectrometry. Using the fluorescent dye that was linked to maleimide, we exposed both the wild-type and SSS mutant to the thiol-specific dye, took the labeled protein, denatured it, reduced it and capped the resulting free cysteines with iodoacetamide. Fragments were then trypsinized and the peptides sent in for MS/MS analysis (UC Davis). We were expecting the data to come back with cysteine residues that were either labeled with the fluorescent dye or iodoacetamide. Any cysteine that contained the fluorescent dye would denote the potential location for the free sulfhydryl in the mutant fragment.

However, the MS/MS processing of the protein proved to be challenging. While we attempted different variations of mass spec processing, we were unable to see the first labeling of the protein, despite the clear difference in labeling between the wild-type and mutant fragments (Fig 5D). We still do not know why this failed but we came back to the TB4 domain and its structural composition for further review. Within TB4, there are 8 cysteine residues that could have reshuffled in the mutant background (Fig 5A). However, analysis of the entire protein sequence for the fragment that was purified showed that there are 52 cysteine residues, all sequestered within disulfide bonds. Published work on fibrillin-1 has shown that destabilizing the structure of one domain has the capacity to destabilize the structure of flanking domains and affect the overall capacity of the protein to form microfibrils within the ECM (11). Hence, in the SSS mutant background, the cysteine mutation might not just be affecting the structure of TB4 but could be destabilizing the entire protein structure of the fibrillin fragment.

To determine if that was the case, we completed a more simplified processing of the protein. We took the wild type and mutant fragments and labeled them with iodoacetamide in a non-reduced state. The trypsinized peptides were again sent for MS/MS analysis. This time the results showed that the mutant fragment is easily labeled with iodoacetamide in comparison to the wildtype (Fig 6). Overall, the cysteine residues within the SSS mutant appear to be easily labeled across the entire protein sequence, suggesting that it's in a more reduced state. Because the labeling did not localize specifically to any domain or residue, this suggested that the free sulfhydryl in the SSS mutant fragment is not at the same amino acid position in each protein monomer, instead each monomer may contain a free cysteine anywhere along the protein sequence.

Overall, these results suggest that the SSS mutation destabilizes the entire protein fold of fibrillin-1 and that this change in tertiary structure is responsible for the differential binding of the RGD-binding integrins. In wild-type fibrillin-1, the fragment used for cell adhesion assays contains an even number of cysteine residues that are all included in disulfide bonds, leaving no free sulfhydryls, as confirmed by fluorescent labeling and DTDP reactivity. The mutation of a highly conserved tryptophan to cysteine within the RGD-containing TB4 domain could easily prompt disulfide shuffling given its key role in stabilizing the hydrophobic core of this domain. Furthermore, the WC mutation removes the tryptophan that forms the hydrophobic core of domain TB4 and replaces it with an additional cysteine, which could remain as a free sulfhydryl, initiate dimerization of the fragment or cause a misfold with a free thiol that is inaccessible. Coomassie staining of the mutant in non-reduced conditions as well as reactivity with DTDP, confirmed the presence of a single cysteine which remained free but did not result in protein dimerization. The ease with which the mutant fragment is labeled by thiol-reactive species further suggests that the tryptophan to cysteine mutation in SSS destabilizes the entire protein fold of fibrillin-1. This reduced state of the mutant could potentially explain why our initial mass spec analysis did not work. We were assuming that each mutant fragment contained the same free cysteine at the exact same location but looking at how the protein behaves in a non-reduced state provides support for the hypothesis that the whole structure of the mutant protein is disrupted. Unfortunately, this will be challenging to confirm and the current mass spec tools

required to answer this question are not available. However, it does suggest that the SSS mutation is causing the reshuffling of disulfide bonds across multiple domains of fibrillin-1, generating a variety of free sulfhydryls.

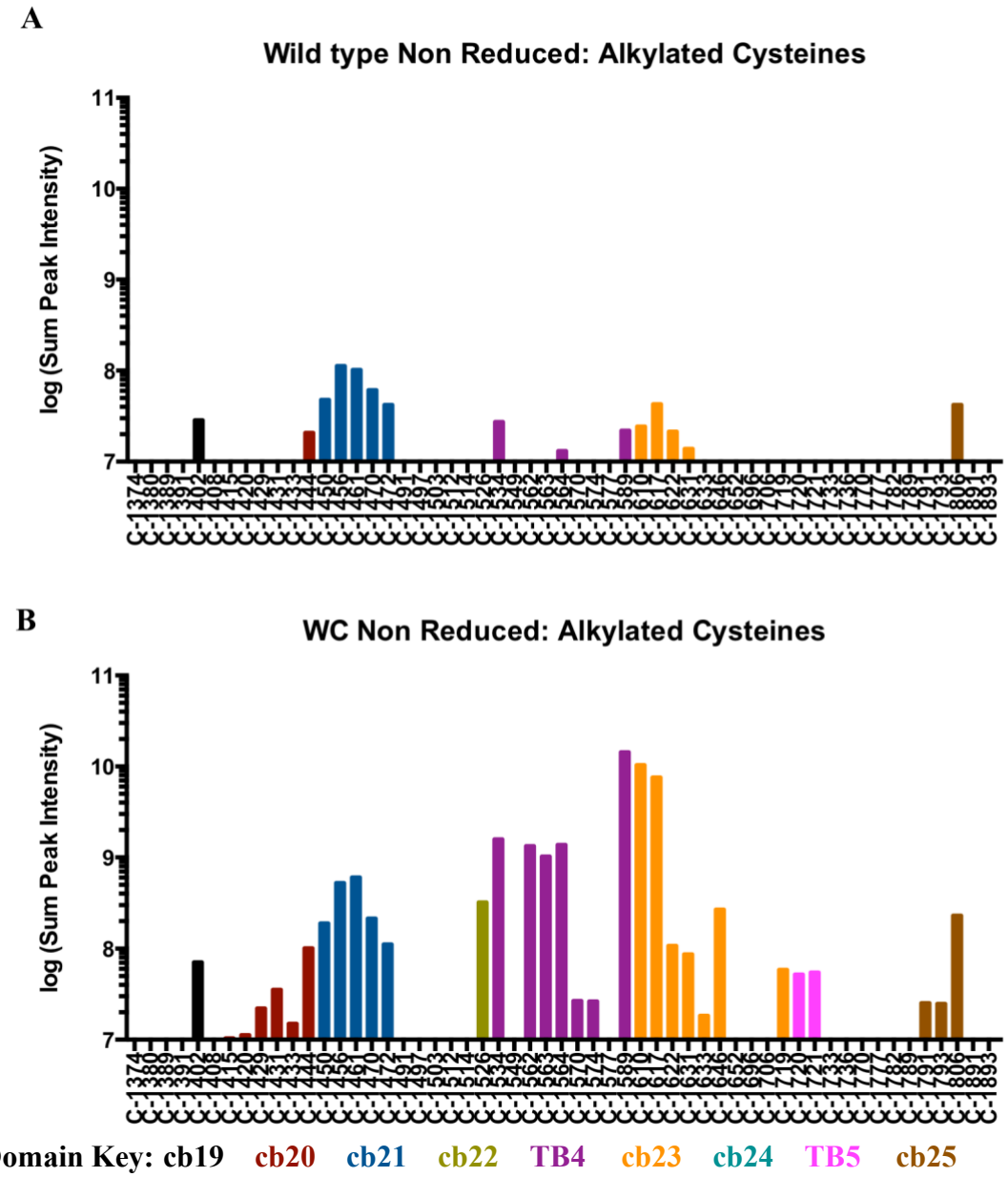


**Figure 6. Alkylation of Fibrillin-1 shows Increased Reduction of the SSS Mutant:** **(A)** Non-reduced wild-type fibrillin-1 was labeled with iodoacetamide, trypsinized and peptides submitted for MS/MS analysis to UC Davis. Alkylated cysteine residues are identified by peak intensity of each peptide containing the labeled residue. X-axis: cysteine residues in fibrillin-1 fragment cbEGF19-cbEGF25. Y-axis: log sum of peak intensity for each labeled peptide. **(B)** Non-reduced SSS fibrillin-1 containing the tryptophan to cysteine mutation was labeled with iodoacetamide, trypsinized and peptides submitted for MS/MS analysis to UC Davis. Alkylated cysteine residues are identified by peak intensity of each peptide containing the labeled residue.

Chapter Four

## The SSS mutation results in increased TGFβ activity

TGFβ has been implicated as an important regulator of almost all major cell behaviors and activities, including proliferation, adhesion, motility, apoptosis and differentiation (40). Its control of multiple signaling and transcriptional events allows TGFβ to promote synthesis and inhibit degradation of the ECM, leading to the accumulation of ECM that is characteristic of fibrosis (41). This critical role of TGFβ in fibrotic disease progression has implicated the cytokine, its receptors and its activators as potential targets for drug therapy.

In the context of SSS, a pan-specific blocking antibody of TGFβ (1D11) was shown to reverse the fibrotic phenotype of the SSS mouse model (17). While increased pSMAD levels have been shown to be present in the dermis of patient skin grafts, the method for cytokine activation remains unclear. Aberrant integrin-mediated activation of TGFβ (through binding of the RGD motif in LAP) has been shown in other models of fibrosis to play a critical role in the development of fibrosis. While the previously cited paper examining the *in vivo* effects of an SSS-causing mutation postulated that the increased TGFβ activity seen in SSS was due to enhanced bioavailability of TGFβ (due to poor assembly of fibrillin-1 microfibrils thus affecting the protein's ability to sequester the latent complex), no work was done to evaluate the potential role of integrins as activators of TGFβ (17).

Our cell adhesion assays demonstrated that the W to C mutation in fibrillin-1 differentially affected the ability of the RGD-binding integrins to mediate cell adhesion, in certain instances completely abrogating the ability of specific integrins to bind to the RGD motif in fibrillin-1. These results suggested an alternative pathway to TGFβ activation: loss of integrin binding to fibrillin-1 allows specific integrins to bind to and activate TGFβ. More explicitly, in the wild-type background, high concentrations of fibrillin-1, assembled into functional microfibrils, maintain cell surface integrins bound to the ECM (fibrillin-1), effectively

competing for the ability of these integrins to bind to and activate latent TGFβ. Introduction of the W to C mutation could cause the loss of both integrin binding and proper microfibril assembly allowing the latent

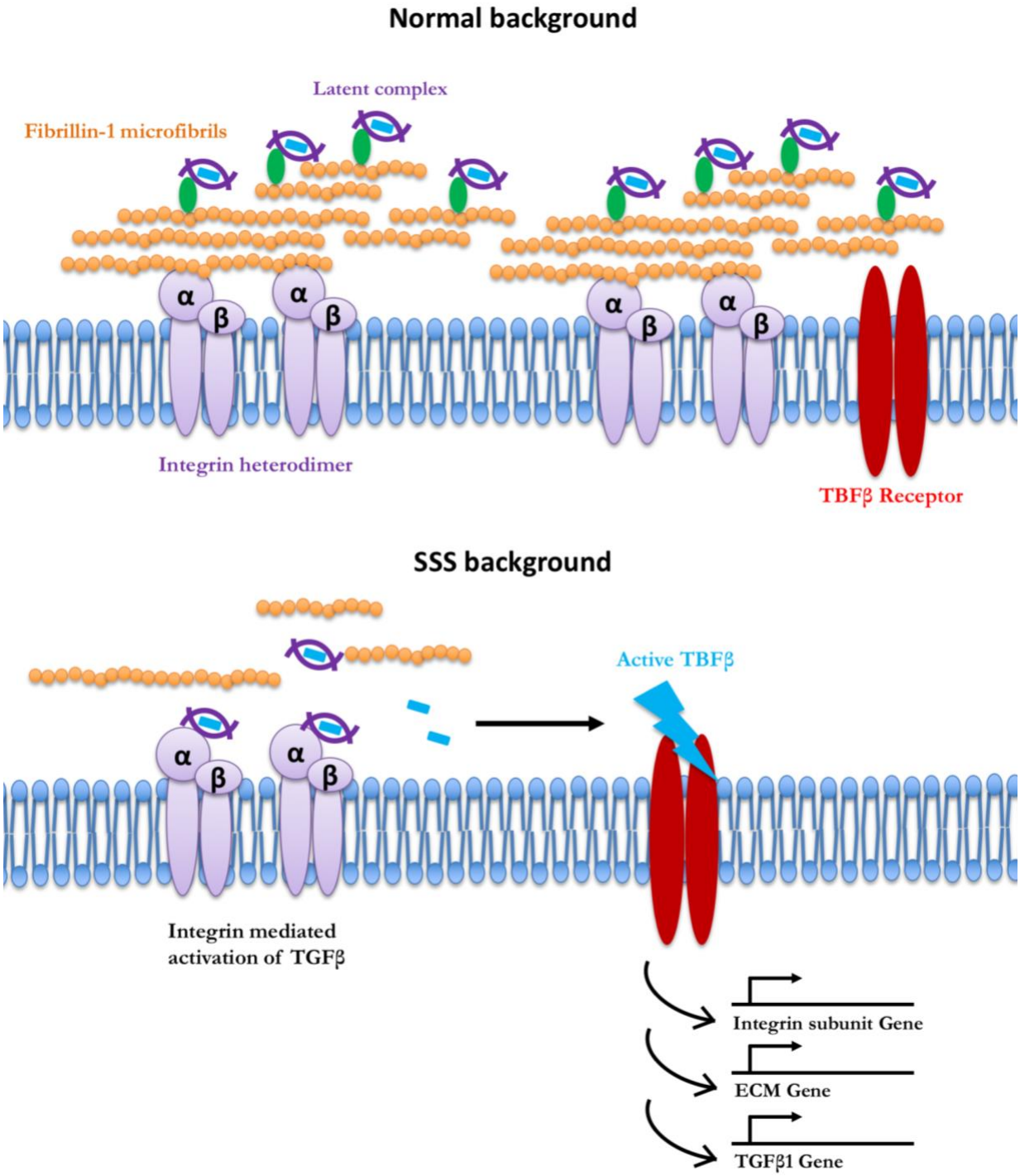


**Figure 7. Schematic of Proposed Mechanism of Action in SSS:** effects of WC fibrillin-1 on integrin-mediated activation of TGFβ and subsequent disease progression.

cytokine and now available integrins to more effectively interact and release active TGFβ, which would then be free to stimulate TGFβ receptors on nearby cells (Fig 7). We sought to test this hypothesis by focusing on the integrins that lost their ability to mediate cell adhesion to fibrillin-1 in the SSS background, αvβ5, α5β1, αvβ6 and αvβ1.

***The SSS mutant shows activation of TGFβ***

To specifically determine the relationship between fibrillin-1, the RGD-binding integrin subfamily and TGFβ, we used a well-established co-culture assay using reporter TMLC cells that have been transduced to express a TGFβ-sensitive portion of the plasminogen activator inhibitor-1 promoter driving firefly luciferase (see methods). Overnight co-culture of TMLC cells with fibroblasts has specifically shown that these cells can active TGFβ and that activation can be abrogated with specific TGFβ blockade (42).

Based on the results from our cell adhesion assays, only integrins αvβ5, α5β1, αvβ6 and αvβ1 lose their ability to mediate cell adhesion to fibrillin-1 in the diseased SSS background. Of these four integrins, only αvβ1 and αvβ6 have previously been shown to activate TGFβ through specific LAP binding to the latent complex. We focused on studying αvβ1 since small molecule blockade of this integrin has previously been shown to reduce the progression of fibrosis in multiple organs (34). Furthermore, αvβ6 is an epithelial-specific integrin that is not expressed on the cell surface of fibroblasts and is only minimally expressed on keratinocytes. Since the fibrosis seen in SSS generally occurs in the lower part of the dermis, far away from the keratinocytes, we did not consider αvβ6 to be a likely activator of TGFβ in this model. (However, we did treat SSS mice with αvβ6 blocking antibody (3G9) and saw no effect, (data not shown).)

We co-cultured two different cell lines that express αvβ1 with the TMLC reporter cells: CHOαv, Chinese hamster ovarian cells that have been transduced to over-express the human αv subunit and thus express a chimeric αvβ1 on the cell surface and WI38 lung fibroblasts that endogenously express αvβ1. Both cell lines were plated on high concentrations of all three fibrillin-1 fragments (30μg/ml) containing collagen-1a to ensure cell adhesion in the context of the SSS and RGE mutants. The co-culture assay was

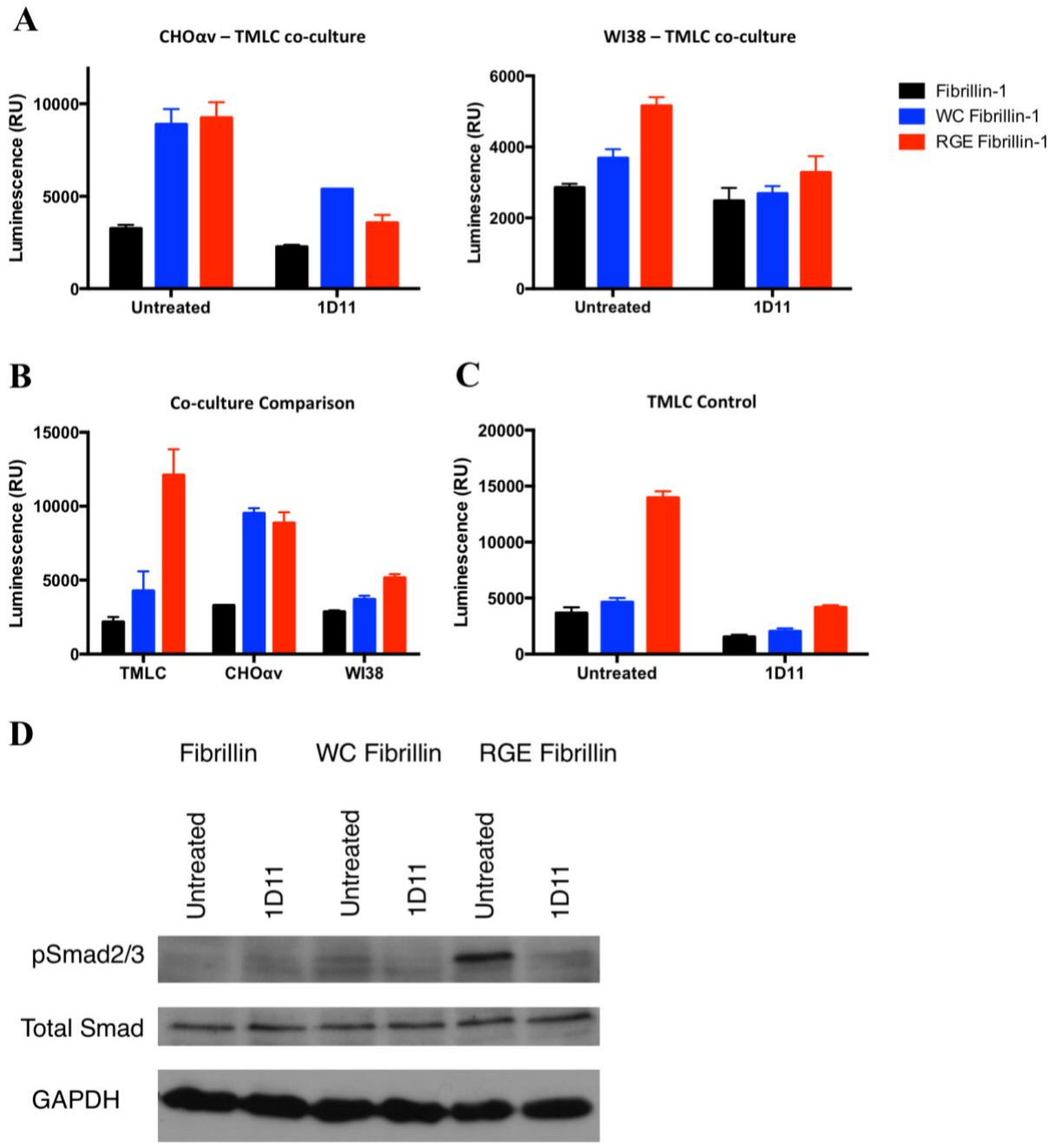


**Figure 8. SSS Mutant Fragment shows Increased TGFβ Activation:** **(A)** Co-culture assays of CHOαv and WI38 cells plated overnight with TMLC reporter cell line on high concentrations of wild-type, WC and RGE fibrillin-1 in the presence of collagen 1a. Cells were plated either in the presence or absence of 1D11, a pan-specific blocking antibody against TGFβ. (**B)** The TMLC reporter assay completed on all three fibrillin-1 fragments as described above under untreated conditions for TMLC cells alone, co-cultured with CHOαv and co-cultured with WI38. **(C)** Blockade with 1D11 of TMLC coated alone on fibrillin-1 plates. Graphs were generated from a mean of 3 replicates, with SEM. **(D)** Western blot analysis of pSMAD2/3, total SMAD and GAPDH from WI38 lung fibroblasts plated on wild-type, WC and RGE fibrillin-1 fragments in the presence of collagen 1a. Cells were allowed to grow for 2 hrs at 37° either untreated or in the presence of 50μg/ml 1D11. Cells were lysed with RIPA buffer and 100 μg of total protein run on a 12% SDS-PAGE.

allowed to grow overnight in the presence or absence of 1D11, a pan-specific TGFβ-blocking antibody. Cells were then lysed and quantified for expression of luciferase.

The co-culture assay for both CHOαv and WI38 cells showed increased TGFβ activation, as measured by luciferase activity, on cells plated on WC and RGE fibrillin-1 fragments. That activation was significantly blocked in the presence of 1D11, a pan-specific TGFβ blocking antibody (Fig 8A). These results are consistent with previous data that has shown increased TGFβ activity in the SSS background. However, these results were confounded not by the luciferase activity seen with TMLC cells plated on wild type fibrillin (many cells reduce basal TMLC activity) but by the fact that reporter cells by themselves also appear to activate TGFβ when they are plated on the mutant fragments (Fig 8B). This activation was especially apparent when TMLC cells were plated on the RGE loss-of-integrin binding fragment. Furthermore, the activation of TMLC cells alone on WC and RGE fibrillin-1 was blocked by incubation with 1D11, suggesting that luminescence observed was indeed due to increased TGFβ activity in TMLC cells and not due to an alternate activation pathway for the PA1 promoter (Fig 8C). Because TMLC reporter cells plated on non-RGD integrin ligands, such as collagen-1, do not activate TGFβ, it was not possible to infer that loss of the sequestration of an RGD-binding integrin was responsible for this effect.

We therefore repeated these experiments with a simpler system that did not require reporter cells, using phosphorylation of SMAD2, an early read out of TGFβ signaling activity, as our indication of TGFβ activation. WI38 fibroblasts were plated on high concentrations of fibrillin fragments in the presence of collagen-1a as completed for the co-culture assays and incubated at 37° for 2 hrs. Cells were lysed for western blot detection of total SMAD2/3 and phospho-SMAD2/3. In this experiment, we saw an increase in pSMAD2 in cells plated on either mutant form of fibrillin-1 (WC or RGE), with the largest effect on the RGE mutant (Fig 8D). These results are consistent with our hypothesis that loss of binding to the RGD site in fibrillin-1 could potentially lead to increased TGFβ activation by primary fibroblasts.

***The SSS mouse model suggests potential role for integrin αvβ1 in disease progression***

The SSS mouse model described above showed increased collagen deposition in the dermis as well as decreased subcutaneous fat that resulted in overall increased skin thickness by three months of age. This fibrosis phenotype was normalized through the use a pan-specific TGFβ neutralizing antibody and thus suggested that disease progression was dependent on TGFβ activity. To determine if αvβ1 mediated TGFβ activation in these mice, we treated W1572C (mouse equivalent of the human W1570C SSS mutation) fibrillin-1 mutant mice with the αvβ1 integrin inhibitor c8, a small molecule that was designed in collaboration with Bill DeGrado at UCSF and has been shown to attenuate αvβ1-mediated activation of TGFβ in pulmonary and liver fibrosis (24).

We treated both control and SSS mice with the c8 inhibitor, delivering the inhibitor (or control di-peptide, c16) by continuous infusion Alzet pumps for 8 weeks. We determined whether pharmacological inhibition of αvβ1 normalized the fibrosis phenotype by taking a clinical score of skin stiffness and measuring the stretched skin area/total surface (SSS/TSA), where the ratio provided a measurement of skin thickness. Clinical scores were taken by five observers blinded to genotype and treatment status (Fig 9A). Mice were assessed in random order, where a score of 1 indicates no stiffness (i.e., identical to wild-type mice) and a score of 4 indicates extreme stiffness. Scores of 2 and 3 indicate a subjective assessment of an intermediate level of stiffness. While the data showed a significant difference between the clinical scores of wild-type and SSS mice, treatment with the c8 inhibitor did not normalize the scores. However, there was a significant difference between the treated vs. untreated SSS mice, albeit a small change in scoring. This difference suggested that inhibition of αvβ1 integrin results in partial protection against fibrosis, potentially by preventing the integrin-mediated activation of TGFβ. These results however were not reflected in any of the other measurements we made (data not shown).

The SSA/TSA ratio showed that mutant mice treated with the c8 inhibitor failed to normalize back to wild-type levels, although there was a trend toward improvement (Fig 9B). The skin thickness of these SSS mice also failed to normalize upon treatment of c8 (data not shown). Measurements for hydroxyproline

levels in the dermis showed no difference between wild-type and SSS mice, regardless of drug treatment. These results suggest that αvβ1, at best, plays a small role in driving fibrosis in the SSS mice.

There are limitations however to the interpretation of these results. While the data published by Gerber, et al, in 2013 from the SSS mouse model showed convincing development of skin thickening and stiffness, the magnitude of this effect was not as large in the mice we bred onsite at UCSF. Furthermore, Gerber, et al used heterozygous W1572C mice, in which his group was able to show clear differences between the wild-type and mutant mice. Our experiments, however, had to be completed using homozygous $Fbn1^{W1572C/W1572C}$ mice. In unpublished data from the group who originally developed the model (Hal Deitz, personal communication) they also found diminished responses over time in their facility, effects they hypothesized might have depended on alterations in the gut microbiome. While they did not report analysis of hydroxyproline content in the dermis, our lab was unable to demonstrate differences between the wild-type and diseased mice for this critical fibrotic measurement. The results we did observe leave open the possibility that αvβ6 and αvβ1 might cooperate in activating TGFβ in this model or that TGFβ activation occurs by both integrin dependent and independent mechanisms.

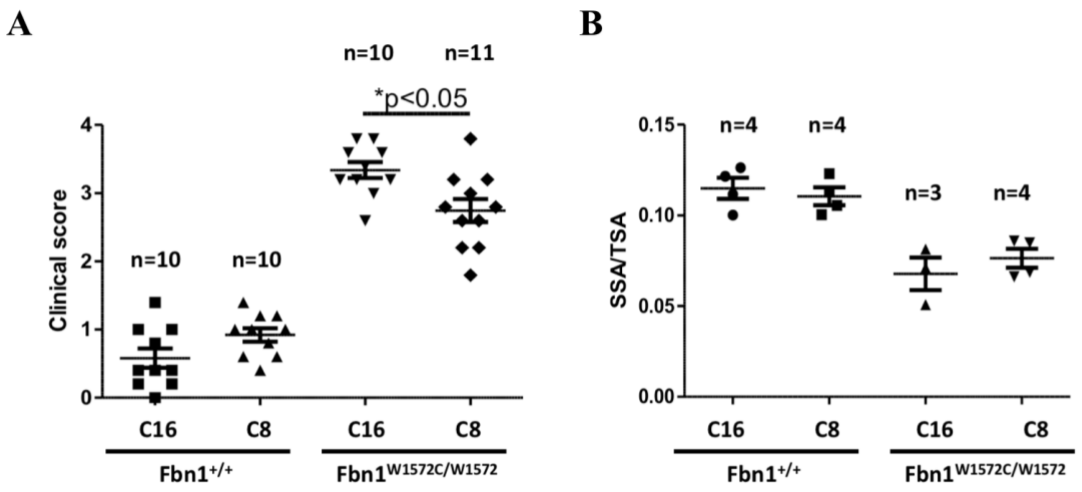


**Figure 9. *In-vivo* Treatment of SSS Mice with αvβ1 Small Molecule: (A)** Clinical score of wild-type and SSS mice treated with either the control (c16) or c8 inhibitor against αvβ1. Measurements were taken after 8 weeks of treatment and is a mean of two experimental cohorts. (**B)** Measurements of stretched skin area/total skin area (SSA/TSA) were taken after 8 weeks of treatment. Mice were euthanized and their back-hair removed. Mice were then briefly suspended by their back skin and photographed in profile in a uniform manner.

Chapter Five

## Discussion and Future Directions

While the original goal of this work was to determine the relationship between fibrillin-1, the RGD-binding integrin subfamily and TGFβ in causing Stiff Skin Syndrome, further work remains to be done to fully understand the development of this form of scleroderma. Our results suggest that loss of binding of one or more of the 4 integrins whose adhesion was inhibited by the disease-causing mutation (α5β1, αvβ1, αvβ5 and αvβ6) likely play(s) a role in the development of SSS. We have not excluded the possibility that SSS is caused, at least in part, by enhanced activation of TGFβ by αvβ1 and αvβ6, but the lack of effect of the αvβ6 blocking antibody, 3G9 and the minimal effect of the αvβ1 inhibitor, c8, suggest that any role of this pathway may be minimal, at best.

It is important to note that all the missense mutations that result in the specific develop of SSS are due to either the addition or deletion of a cysteine residue within TB4 (16). The strict correlation between the gain or loss of this amino acid residue and its free thiol group to the development of SSS strongly suggests that the disease progression is due to altered disulfide bond formation. It is this loss of proper protein folding that ultimately results in a significant change in the conformation of the TB4 domain, affecting the structural context of the exposed RGD site and the overall function of fibrillin-1. Rearrangements in the internal conformation of TB4 would further lead to alterations in tertiary structure, which are the probable explanation for differential loss of adhesion mediated by RGD-binding integrins to this domain.

A functional RGD sequence is defined by a flexible loop that allows for a conformation in which the side chains of the tripeptide are pointed out in almost opposite directions (43-44). The outward extension of the motif allows for ease of accessibility by RGD-binding receptors; tertiary or quaternary structures that result in the burial of the RGD sequence will not interact with the integrin binding pocket. Furthermore, the amino acids following the RGD-domain have been shown to have significant differential effect on the ability to mediate robust integrin binding. Peptides containing glycine, tryptophan or

phenylalanine following the RGD motif are easily recognized by α5β1 (45). Substitution of serine or alanine in those sites results in preferential binding by αvβ3 and αvβ5. An even more specific peptide containing tyrosine or arginine results in highly potent recognition by αIIbβ3 (46). Not only is the immediate flanking sequence of the RGD motif important for integrin binding, the positioning of a ligand's secondary structure can also have a dramatic effect. For example, integrins α5β1 and αvβ3 are both known receptors for mediating cell adhesion to fibronectin (FN). While αvβ3 recognizes the RGD motif in the $10^{th}$ type III repeating unit of FN, α5β1 requires a synergy site in the $9^{th}$ type III unit, PHSRN (47). Absence of this amino acid sequence results in a substantial loss of binding by α5β1 but does not affect the binding capacity of αvβ3. These differences in recognition demonstrate the importance of FN topology for receptor binding to the RGD site (48-49). Fibrillin binding to αvβ3 and αvβ6 has also been shown to be dependent on domain context. αvβ3 requires cbEGF22 together with TB4 to achieve high affinity binding, whilst αvβ6 does not (50).

Although the RGD site of fibrillin-1 is 20 Å removed from the mutated tryptophan-1570 site, it is reasonable to expect the W1570C mutation to influence integrin specificity by both altering the local conformational energy and dynamics of its RGD tripeptide as well as more distant interactions. While our mass spec analysis of the wild-type and mutant fragments did not conclusively determine the structural differences between the two fragments, it did provide the basis for further study into the effects of sulfhydryls on protein structure. Knowing that the SSS fibrotic phenotype of fibrillin-1 only develops when a cysteine residue is either deleted or added to TB4, it would be interesting to see how our cell adhesion results change when tryptophan-1570 is mutated to an alternate residue. Tryptophan-1570 plays an important role in stabilizing the hydrophobic core of TB4 and presumably mutating this residue (to something besides cysteine) would still have an effect on protein fold but should not cause the same dramatic disulfide reshuffling suggested by our MS/MS analysis. It is even possible that this alternate mutation would not have any effect on the ability of the 7 identified integrins to mediate cell adhesion to fibrillin-1. This would further confirm that the structural changes in TB4 (disulfide bridge reshuffling)

imparted by an uneven number of cysteine residues is directly responsible for disease progression. Further confirmation of the structural differences between the two fragments could be identified by solving the crystal structure of the WC fibrillin-1 fragment. Though this experimental approach would only work reliably if the mutant fragment exists in one stable and abundant form, which our MS/MS analysis suggests otherwise. However, if we were able to identify a stable structural form of WC fibrillin-1, the comparison between that structure and the solved crystal structure for the wild-type fragment would highlight the differences in TB4 that presumably change the flexibility and accessibility of the RGD motif. Those results would further demonstrate the importance of secondary and tertiary structure in ligand binding interactions for the RGD-integrin subfamily.

Understanding how our *in-vitro* cell adhesion data translates directly to the disease model is perhaps the most critical step forward in understanding the SSS phenotype. While our system setup provided a clear method through which to evaluate all 8 RGD-binding integrins, our model cell lines did not exclude indirect roles for these integrins in the more complex *in vivo* environment of the skin. Additionally, most of the 7 of the 8 RGD binding integrins were evaluated when their cell surface expression was high due to transfection of the SW480 cells. The data we thus generated would translate only to cells that are also expressing high levels of cell surface integrins. The differences between our system and a more biological imitation of the cell environment in the dermis was seen in HDF. These cells express high levels of $\alpha v\beta 1$ and $\alpha 5\beta 1$ but relatively low levels of $\alpha v\beta 5$ and $\alpha v\beta 3$, as compared to the SW480 cell system (Fig 2). In HDF, $\alpha v\beta 3$ mediated lower levels of cell adhesion to fibrillin-1 and $\alpha 5\beta 1$ mediated high cell adhesion (data not shown), almost in direct contrast to the observed results in the SW480 system. These discrepancies highlight the complexity of the biology that would be at play in the dermis of SSS. The biological differences between cell surface expression of integrins in the disease relevant cells (HDF, infiltrating immune cells, etc.) could help identify a different pattern and/or role for integrins. The effects of the tryptophan to cysteine mutation in fibrillin-1 would perhaps be most importantly evaluated within HDF, as activated fibroblasts have been shown to be the main cell responsible for excessive deposition of ECM

proteins in fibrosis. Completing the integrin profile of HDF on wild-type and WC fibrillin-1 could identify a specific integrin(s), perhaps αvβ1, responsible for regulating the changes in the dermis that lead to fibrosis.

While determining the relationship between fibrillin-1, the RGD-integrin subfamily and TGFβ proved to be challenging, the preliminary data we generated does suggest cross-talk between these three proteins and suggests further work remains to be done. The TGFβ activation assays would have provided a clear and concise method through which to map these interactions, however the ability of TMLC cells to activate TGFβ alone on fibrillin-1 coated plates reduced the credibility of this method. The interference seen in this system was surprisingly unique to fibrillin-1. TMLC plated alone on plastic produce very little TGFβ1 or 3, the isoforms activated by integrins, but it is conceivable that this expression pattern changed when cells were plated on fibrillin-1 fragments. It is interesting to note that the activation pattern of TGFβ by TMLC followed our proposed mechanism - TGFβ was activated to higher levels when cells were plated on the WC mutant and RGE-loss of integrin binding fragments. While the cell system is not directly applicable to our model (TMLC being mink lung epithelial cells), it does suggest that with the right cell system, we could indeed measure the changes in TGFβ activation in this disease background. Indeed, preliminary western blots do show that coating lung fibroblasts on the fibrillin-1 fragments results in a change in phosphorylation of SMAD2/3. Increased levels of pSMAD2/3 in cells coated on WC and RGE fibrillin is consistent with the literature and the development of fibrosis in SSS mice. Further studies using specific integrin blocking antibodies (anti-αv, anti-β1, etc.) and small molecular inhibitors such as c8 would clarify if the observed TGFβ activity is directly due to integrin-mediated activation. If further study were to show that phosphorylation of SMAD2/3 on WC and RGE fibrillin-1 can be prevented by blocking integrin receptors, specifically αvβ1, it would provide some support to the hypothesis that the loss of integrin binding to fibrillin-1 results in the fibrotic phenotype of SSS through activation of TGFβ.

Those results would warrant further inquiry into the SSS mouse model, specifically why the c8 inhibitor failed to normalize skin stiffening. Though our results in the SSS mouse model showed that αvβ1 did affect the phenotype of these mice through observed clinical stiffness scores, the magnitude of this

protective effect was not large. However, one limitation of our *in vivo* studies is that we cannot be certain that the antibody and small molecule we used were present at sufficient concentrations in the dermis to completely inhibit TGFβ activation or that they obtained sufficient access to the sites of cell-cell contact where integrin-mediated activation of TGFβ occurs. These issues could be addressed in future studies by specifically measuring the drug and antibody levels in dermal tissue of treated and untreated animals and by assessing pSMAD2/3 by western blotting or immunostaining.

In addition to αvβ1, we completed similar testing of αvβ6 through antibody specific blockade using 3G9 and again saw no changes in the fibrotic phenotype of treated vs untreated mice (data not shown). This result is consistent with the fact that αvβ6 expression is limited to epithelial cells and levels of expression are generally quite low in the skin. While the direct effect of integrins in fibrotic disease progression has been previously identified through the use of genetic tools (knockout of α or β subunits), this method of approach cannot be used for αvβ1. Global loss of either αv or β1 integrin subunit result in embryonic lethality and neither knockout is specific for αvβ1. This genetic approach can however be used to either include or exclude a potential role for αvβ6 by crossing SSS mice to β6 knockout mice. If these double mutant mice (SSS and β6 ko) develop fibrosis, even in the setting of αvβ1 inhibition, these findings would suggest that αvβ6 does not play a prominent role in the activation of TGFβ in SSS. While the αv and β1 global knockout mice cannot be evaluated, we can specifically assess the role of all αv integrins in fibroblasts using PDFGRβ-CRE mice crossed to αv flox/flox mice, as we have previously done to study lung, liver and kidney fibrosis. If our hypothesis holds true then these mice are expected to be protected from disease progression and would thus confirm that an αv integrin is responsible for the development of fibrosis in SSS. Specifically, this would suggest that αvβ1 and/or αvβ5 binding to fibrillin-1 is critical for maintaining normal cell-matrix interactions, assuming αvβ6 is eliminated as a potential factor.

Our results also leave open the possibility that loss of binding of α5β1 or αvβ5 also contribute to the SSS phenotype through a mechanism that does not involve direct integrin-dependent TGFβ activation. Our lab has generated the global knockout of integrin β5, which is effectively a specific knockout of αvβ5,

but see no signs of skin stiffness in these mice. However, it is conceivable that loss of αvβ5 binding and aggregation of mutant fibrillin by a mechanism independent of integrin binding are both required to see the SSS phenotype. In that case, it is possible that we would see protection from SSS by crossing the integrin β5 knockout mice with SSS mice. A potential role for loss of α5β1 binding is supported by the reported finding that a β1 activating antibody protects SSS mice from skin fibrosis. However, global α5 knockout mice die during embryonic development and while we have mice expressing a conditional α5 allele in the lab, it is not immediately clear in which cell type we should inactivate α5.

Gerber et al did report crossing SSS mice into mice heterozygous for a null allele of the integrin β3 subunit and showed that these mice were protected from disease progression. These results prompted them to speculate a potential role for αvβ3 as a therapeutic target in SSS. In contrast to the effects of the WC mutation on αvβ6, αvβ1, αvβ5 and α5β1, our assay showed that the WC mutation did not affect the ability of αvβ3 to mediate cell adhesion to fibrillin-1. Additionally, αIIbβ3 showed enhanced binding to the mutant fragment. Though the clear observable protection of the β3 null mice crossed to SSS suggests that either αvβ3 or αIIbβ3 play a role in disease progression, it is unclear how or why. Considering that HDF express low levels of αvβ3, it is possible that this protection is due primarily to αIIbβ3 expressed on platelets. Further studies to confirm and understand how knockout of β3 protects SSS mice from fibrotic development remains to be completed. While the PDFGRβ-CRE mice crossed to αv flox/flox mice would suggest potential roles for αvβ3, αvβ5 and αvβ1, the knockout of αIIb in the SSS mice would provide a clear distinction between the two. Though neither the mouse model nor the observed human phenotype have shown any dysregulation of platelet aggregation and function, if the αIIbβ3 mice in the SSS background are also protected from disease progression, as seen in the β3 cross to SSS, it would suggest that αIIbβ3 also plays a prominent role that needs to be further explored. Alternatively, it is entirely possible that αvβ3 expressed on a non-fibroblast cell (infiltrating immune response) is responsible for the protection seen in the β3 heterozygotes, though it might not be due to interactions with fibrillin-1 since this integrin is cable of mediating cell adhesion to both the wild-type and WC fragment with equal strength.

The complexity of integrin biology and its important role in various cell functions highlights the diversity of this protein family. While our work initially set out to identify a primary integrin responsible for mediating cell interactions with fibrillin-1, we clearly showed that the RGD-binding integrins share a more complex relationship with this ECM protein then initially presumed. The development of SSS may not be controlled by changes in the ability of one single integrin to bind fibrillin-1 but by more than one integrin. Eventual treatment of this stiff skin phenotype may require multiple targets, multiple integrins and an even more precise understanding of the microenvironment in the diseased dermis.

Chapter Six

# Methods

***Reagents:***

Purified mouse anti-CD51 (integrin αv) was purchased from BD Biosciences; rabbit anti-integrin β1 was purchased from Millipore; ChromePure Mouse IgG was purchased from Jackson ImmunoResearch. Anti-αv mouse monoclonal antibody, L230 (51), was purified in our lab from a hybridoma obtained from ATCC. Anti-α5β1 mouse monoclonal antibody, P1D6, was a generous gift from Elizabeth Wayner (Fred Hutchinson Cancer Center). Anti-αIIbβ3 mouse monoclonal antibody, 10E5 was a generous gift from Barry S Coller (Rockefeller University). Anti-α8β1 mouse monoclonal antibody, YZ83 was a generous gift from Yasuyuki Yokosaki (Hiroshima University). Mouse monoclonal antibodies against αvβ5 (ALULA), αvβ3 (AXUM2) and αvβ8 (ADWA-11) were generated in our laboratory and anti-αvβ6 mouse monoclonal antibody, 3G9, was a generous gift from Biogen Inc. 4,4'-dithiodipyridine was purchased from Sigma-Aldrich and Alexa-Fluor™ 647 $C_2$ maleimide was purchased from Invitrogen.

***Cells*:**

Human dermal fibroblasts (HDF) and growth kit medium were purchased from ATCC and cultured according to the vendor's instructions. Colon carcinoma SW480 cells were used to generate transfected cell lines that overexpressed integrin subunits, α8, β3, β6, and β8, as previously described (52-55)

***Isolation of human platelets:***

Whole blood was drawn using a plastic syringe containing 1/10 volume CPD buffer (15 mM citric acid, 90 mM sodium citric, 16 mM $Na_2H_2PO_4$, 142 mM D-glucose, pH 7.4) with 1 μM PGE-1. Cells were mixed gently, transferred to a 50 mL conical and spun at 200xg for 15 min, room temp. The top layer containing the platelet-rich-plasma was transferred to a new 15 mL conical containing 1/10 volume of buffer ACD (39

mM citric acid, 75 mM sodium citric, 135 mM D-glucose, pH 7.4). PGE-1was added to a final concentration of 0.4 μg/mL to prevent platelet activation. Cells were pelleted by centrifugation at 800xg for 20 min at room temp. Platelets were rinsed with wash buffer (10 mM sodium citric, 150 mM NaCl, 1 mM EDTA, 1% D-glucose, pH 7.4) without resuspension to avoid unnecessary activation. Cells were carefully resuspended in 5-10 mL of HEPES-Tyrodes's buffer (134 mM NaCl, 12 mM $NaHCO_3$, 2.9 mM KCl, 0.34 mM dibasic $Na_2HPO_4$, 1 mM $MgCl_2$, 1 mM $CaCl_2$ 10mM HEPES, 5 mM glucose, 1% BSA, pH 7.4). For use in adhesion assays, platelets were activated using PAR-1 at a final concentration of 100 μM.

***Immunoprecipitation:***

HDF and SW480 cells were lysed in 50 mM Tris-HCl, pH 7.5, 10 mM $MgCl_2$, 150 mM NaCl and 1% Triton X-100, with protease and phosphatase inhibitor cocktail (ThermoScientific). Lysates were centrifuged and total protein concentration determined using Pierce BCA Protein Assay Kit. Samples were incubated with integrin αv antibody, L230, for 1 hr at 4°C with rotation (70 rpm). Protein G Sepharose (GE Healthcare) beads were then added with a further 1 hr incubation. Samples were washed four times with 1 mL lysis buffer and eluted with reducing sample buffer, resolved by SDS-PAGE, and analyzed by immunoblot.

***Flow cytometry:***

HDF and SW480 cells were collected from 10 cm dishes with 0.05% Trypsin-EDTA and washed twice with PBS. 1 x $10^6$ cells were re-suspended in PBS supplemented with 1% BSA and then incubated with primary antibody at 4°C for 1 hr. Cells were washed twice with PBS before incubation with secondary antibody conjugated to phycoerythrin (PE; Jackson ImmunoResearch). Cells were washed twice with PBS before analysis on a BD FACSCantoll. Antibodies were used at a final concentration of 1 μg/mL as follows: anti-integrin β3 (AXUM2), anti-integrin β6 (3G9), anti-integrin β5 (ALULA) and anti-integrin αv (L230). A chicken anti-integrin α8 (YZ83) antibody was used at 2 μg/mL (generous gift from Dr. Yasuyuki Yokasaki) and anti-integrin α5 (P1D6) was used at 1 μg/mL.

***Cell adhesion assay:***

96-well flat-bottomed Immulon 4HBX microtiter plates (ThermoScientific) were coated with a series of fibrillin-1 protein concentrations diluted in DPBS and then incubated at 37° C for 1 hr. Wells were washed with DPBS before blocking with 2% BSA prepared in DPBS at 37° C for 1 hr. Cells were detached from confluent 10 cm dishes using 0.05% Trypsin-EDTA and re-suspended in serum-free DMEM. Wells were plated with $5 \times 10^4$ cells. For blocking conditions, cells were incubated with 10 μg/mL of indicated antibody (Table 1) for 10 min at 4°C before final plating. Plates were centrifuged at 300 rpm for 5 min prior to a 1 hr incubation at 37°C in a 5% $CO_2$ humidified incubator. Non-adherent cells were removed by centrifugation (top side down) at 500 rpm for 5 min. Remaining adhered cells were stained with 0.5% crystal violet, 0.1% formaldehyde and wells subsequently washed with PBS. The relative number of cells in each well was determined after solubilization in 40 μL of 2% Triton X-100, absorbance was read at 595 nm in a microplate reader (Bio-Rad Laboratories). All determinations were carried out in triplicate.

***Expression and protein purification:***

The pSecTag2A plasmids containing cbEGF19-cbEGF25 of wild-type fibrillin-1 and the disease-causing mutation (WC) were generously provided by Dr. Penny A. Handford. Mutagenesis of this plasmid was completed using QuickChange Site-Directed Mutagenesis Kit to generate the RGE fibrillin-1 fragment. Nucleotide 1543 was mutated to generate a D to E substitution. All three protein fragments contained a His-tag for purification on the C-terminus and were expressed in HEK293FS cells; a 1 L volume of $1 \times 10^9$ cells was transfected using 1 mg of DNA (293Fectin™, ThermoScientific). Cells were allowed to grow for 5 days before medium was collected and diluted 3-fold in 50 mM Tris, pH 8, 200 mM NaCl (resuspension buffer) in a Schott bottle. $Ni^{2+}$-charged chelating sepharose beads (ThermoScientific) were prepped in resuspension buffer before adding to diluted medium and incubated at 4°C for 4 hr with gentle shaking. Sepharose beads were packed into a 10 mL column, washed with 50 mL of cold wash buffer (10 mM imidazole, 50 mM Tris pH 8, 200 mM NaCl). Protein was eluted with 20 mL of cold elution buffer (300

mM imidazole, 50 mM Tris pH 8.0, 200 mM NaCl). 1 mL fractions were collected and run on 10% SDS-PAGE to determine elution of protein. Fractions were dialyzed at 4°C into resuspension buffer using a Slide-A-Lyzer Dialysis Cassette (Pierce). Final protein concentration was determined using a BCA Protein Assay Kit (Pierce) and fragments were stored at 4°C in 0.1% sodium azide.

***Quantification of protein thiols with DTDP:***

Protein samples were adjusted to a volume of 250 μL in DPBS containing 2% SDS and denatured for 15min. Samples were added to 2.5 mL of reaction buffer (100 mM $NaH_2PO_4$, 1 mM EDTA, pH 8). Samples were vortexed and incubated at room temp for 5 min after the addition of 50 μL 4 mM DTDP. Absorbance at 324 nm was read against a water blank (1 cm light path). Absorbance values were corrected using an additional DTDP blank. The amount of free sulfhydryl from solution in the spectrophotometric cuvette was calculated according to E = (A)/ bc where A = absorbance, b = path length in centimeters and c = concentration in moles/liter of SH. The molar extinction coefficient for DTDP in this buffer system is 21,400 $M^{-1}$ $cm^{-1}$. Final concentrations were determined by adjusting for the dilution factor of the 2.8 mL reaction volume.

***Fluorescent labeling with Alexa-Fluor™ 647 $C_2$ maleimide:***

Protein samples were diluted to 0.2 mg/ml in 100 mM Tris·HCl, pH 7. Alexa-Fluor™ 647 $C_2$ Maleimide was added to a final concentration of 0.5 mM and samples were incubated in the dark at room temp for 30-60 min. Labeled fragments were run on a 4-12% Tris-glycine SDS-PAGE and imaged using the 650-laser line.

***MS/MS analysis of non-reduced protein fragments:***

Protein samples were diluted to 0.2 mg/ml in 100 mM Tris·HCl, pH 7. Alexa-Fluor™ 647 $C_2$ Maleimide was added to a final concentration of 0.5 mM and samples were incubated in the dark at room temp for 30-

60 min. Excess dye was removed using Amicon Ultra-0.5 Centrifugal Filter Unit (Millipore Sigma) with a 30-kDa molecular weight cut off. Samples were denatured using 8 M urea and reduced using DTT in molar excess. Resulting reduced cysteines were capped with iodoacetamide at a final concentration of 10mM for 15min. Protein samples were trypsinized overnight and then sent to UC Davis for MS/MS analysis.

***Lucerifase-TGFβ activation assay:***

Test cells were plated at 50,000 cells per well in 96-well plates together with mink lung epithelial cells expressing firefly luciferase downstream of the TGFβ-sensitive portion of the plasminogen activator inhibitor 1 promoter (15,000 to 25,000 cells per well) (42). Cells were cocultured for 16 hours, washed with PBS and then lysed with 1X lysis buffer diluted from Luciferase Cell Culture Lysis 5X Reagent (Promega). TGFβ activity was calculated by measurement of luminescence in the presence and absence of TGFβ blocking antibody 1D11 at 30 μg/mL.

***Mice:***

All mice were cared for in strict compliance with the Animal Care and Use Committee of UCSF. $Fbn1^{W1572C/+}$ mice were generously donated by Hal Dietz from John Hopkins. All experimental mice were on a mixed C57BL/6J background. To minimize potentially confounding background effects, all comparisons between genotypes and between treatment arms within a genotype were made between sex-matched littermates; no other randomization procedures were applied. Sample size estimates for the assessment of therapeutic responses were based on the penetrance and severity of the specific parameter under consideration in untreated cohorts.

***In vivo drug treatment:***

Male mice were treated with c8, c16 (each dissolved in 50% DMSO) or anti-β6 (3G9) at 10 mg/kg through continuous infusion by Alzet osmotic pumps (Durect). Treatment was initiated at 1 month of age and continued for 8 weeks.

***Stiffness scoring:***

A clinical stiffness score was assigned by five observers blinded to genotype and treatment status. Mice were assessed in random order. A score of 1 indicates no stiffness (that is, identical to wild-type mice). A score of 4 indicates extreme stiffness based on previous experience with untreated SSS mice; 2 and 3 indicate a subjective assessment of an intermediate level of stiffness. Early in the course of studies, the same mice were assessed by the same observer on a different day. This pilot demonstrated excellent intra-observer concordance. To measure stretched skin area and total surface area, mice were anaesthetized with isoflurane, and the back skin was shaved and treated briefly with Nair cream. Mice were then suspended briefly with forceps secured to the back skin by a clamp and photographed in profile in a uniform manner.

## References


1. Sakai, L.Y., Keene, D.R. and Engvall, E. (1986) Fibrillin, a new 350-kD glycoprotein, is a component of extracellular microfibrils. *J. Cell Biol.* **103**, 2499-2509
2. Ramirez, F., and Dietz, H.C. (2007) Fibrillin-Rich Microfibrils: Structural Determinants of Morphogenetic and Homeostatic Events. *J. Cell. Physiol.* **213**, 326-330
3. Jensen, S., Robertson, I.B., and Handford, P.A. (2012) Dissecting the Fibrillin Microfibril: Structural Insights into Organization and Function. *Structure.* **20**, 215-225
4. Ramirez, R., and Saki, L.Y. (2010) Biogenesis and function of fibrillin-1 assemblies. *Cell Tissue Res.* **339**, 71-72
5. Olivieri, J., Smaldone S., and Ramirez F. (2010) Fibrillin assemblies: extracellular determinants of tissue formation and fibrosis. *Fibrogensis & Tissue Repair.* **3**:24
6. Lee B., Godfrey M., Vitale E., Hori H., Mattei M.G., Sarfarazi M., Tsipouras P., Ramirez F., Hollister D.W. (1991) Linkage of Marfan syndrome and a phenotypically related disorder to two different fibrillin genes. *Nature.* **352**, 330–334
7. Dietz H.C., Cutting G.R., Pyeritz R.E., Maslen C.L., Sakai L.Y., Corson G.M., Puffenberger E.G., Hamosh A., Nanthakumar E.J., Curristin S.M., (1991) Marfan syndrome caused by a recurrent *de novo* missense mutation in the fibrillin gene. *Nature.* **352**, 337–339
8. Gutpa, P.A, Putnam, E.A., Carmical, S.G., Kaitila, I., Steinmann, B., Child, A., Danesino, C., Metcalfe, K., Berry, S.A., Chen, E., Delorme, C.V., Thong, M.K., Ades, L.C., and Milewicz, D.M. (2002) Ten novel FBN2 mutations in congenital contractural arachnodactyly: delineation of the molecular pathogenesis and clinical phenotype. *Hum Mutat.* **19**, 29-48
9. Corson, G.M., Charbonneau, N.L., Keene, D.R., and Sakai, L.Y. (2003) Differential expression of fibrillin-3 adds to microfibril variety in human and avian, but not rodent, connective tissues. *Genomics.* **83**, 461-472

10. Pereira, L., D'Alessio, M., Ramirez, F., R.Lynch, J., Sykes, B., Pangillinan, T., and Bonadio, J. (1993) Genomic organization of the sequence coding for fibrillin, the defective gene product in Marfan syndrome. *Human Molecular Genetics*. **2**, 961-968
11. Handford, P.A. (2000) Fibrillin-1, a calcium binding protein of extracellular matrix. *Biochim. Biophys. Acta.* **1498**, 84-90
12. Roberston, I., Jensen S., and Handford, P. (2011) TB domain proteins: evolutionary insights into the multifaceted roles of fibrillins and LTBPS. *Biochem. J.* **433,** 263-276
13. Yadin, D.A., Robertson I.B., McNaught-Davis, J., Evans, P., Stoddar, D., Handford, P.A., Jensen, S.A., and Redfield, C. (2013) Structure of the Fibrillin-1 N-Terminal Domains Suggests that Heparan Sulfate Regulates the Early Stages of Microfibril Assembly. *Structure*. **21,** 1743-1756
14. Ramirez, F. and Dietz, H.C. (2007) Marfan Syndrome: from molecular pathogensis to clinical treatment. *Curr Opin Cell Biol.* **17**, 252-258
15. Esterly, N.B. and McKusick, V.A. (1971) Stiff skin syndrome. *Pediatrics.* **47**, 360-269
16. Loeys, B.L., Gerber, E.E., Riegert-Johnson, D., Iqbal, S., Whiteman, P., McConnell, V., Chillakuri, C.R., Macay, D., Coucke, P.J., De Paepe, A., Judge, D. P., Wigley, F., Davis, E.C., Mardon, H.J., Handford, P., Keene, D.R., Sakai, L.Y., and Dietz, H.C. (2010) Mutations in Fibrillin-1 Cause Congenital Scleroderma: Stiff Skin Syndrome. *Sci Transl Med.* **2**, 23ra20
17. Gerber, E.E., Gallo, E.M., Fontana, S.C., Davis, E.C., Wigley, F.M., Huso, D.L., and Dietz, H.C. (2013) Integrin-modulating therapy prevents fibrosis and autoimmunity in mouse models of scleroderma. *Nature*. **503**, 126-130
18. Munger, J.S., Harpel, J.G., Gleizes, P.E., Mazzieri, R., Nunes, I., and Rifkin, D.B. (1997) Latent transforming growth factor-β: Structural features and mechanisms of activation. *Kidney Int*. **51**, 1376–1382
19. Moses, H.L., Roberts, A.B., and Derynck, R. (2016) The discovery and early days of TGF-β: A historical perspective. *Cold Spring Harbor Perspect Biol* **8**, a021865

20. Robertson, I.B., and Rifkin, D.B. (2016) Regulation of the bioavailability of TGF-β and TGF-β-related proteins. *Cold Spring Harbor Perspect Biol* **8**: a021907

21. Munger, J.S., Huang, X., Kawakatsu, H., Griffiths, M.J., Dalton, S.L., Wu, J., Pittet, J.F., Kaminski, N., Garat, C., Matthay, M.A., et al. (1999) The integrin $\alpha_v\beta_6$ binds and activates latent TGFβ1: A mechanism for regulating pulmonary inflammation and fibrosis. *Cell* **96**, 319–328

22. Huang, X.Z., Wu, J.F., Cass, D., Erle, D.J., Corry, D., Young, S.G., Farese, R.V. Jr., and Sheppard D. (1996) Inactivation of the integrin β6 subunit gene reveals a role of epithelial integrins in regulating inflammation in the lung and skin. *J Cell Biol* **133**, 921–928

23. Aluwihare, P., Mu, Z., Zhao, Z., Yu, D., Weinreb, P.H., Horan, G.S., Violette, S.M., and Munger, J.S. (2009) Mice that lack activity of $\alpha_v\beta_6$- and $\alpha_v\beta_8$-integrins reproduce the abnormalities of*Tgfb1*- and *Tgfb3*-null mice. *J Cell Sci*. **122**, 227–232

24. Reed, N.I., Jo, H., Chen, C., Tsujino, K., Arnold, T.D., DeGrado, W.F., and Sheppard, D. (2015) The $\alpha_v\beta_1$ integrin plays a critical in vivo role in tissue fibrosis. *Sci Transl Med*. **7**: 288ra79

25. Henderson, N.C., Arnold, T.D., Katamura, Y., Giacomini, M.M., Rodriguez, J.D., McCarty, J.H., Pellicoro, A., Raschperger, E., Betsholtz, C., Ruminski, P.G., et al. (2013) Targeting of $\alpha_v$ integrin identifies a core molecular pathway that regulates fibrosis in several organs. *Nat Med*. **19**,1617–1624

26. Downing, A.K., Knott, V., Werner, J.M., Cardy, C.M., Campbell, I.D., and Handford, P.A. (1996) Solution structure of a pair of calcium-binding epidermal growth factor-like domains: Implications for the Marfan Syndrome and other genetic disorders. *Cell*. **85**, 597-605

27. Sakamoto, H., Broekelmann, T., Cheresh, D.A., Ramirez, F., Rosenbloom, J., and Mecham, R.P. (1996). Cell-type Specific Recognition of RGD- and Non-RGD-containing Cell Binding Domains in Fibrillin-1. *J. Biol. Chem.* **271**, 4916-4922

28. Pfaff, M., Reinhardt, D.P., Sakai, L.Y., and Timpl, R. (1996) Cell adhesion and integrin binding to recombinant human fibrillin-1. *FEBS Letters.* **384**, 247-250

29. Bax, D.V., Bernard, S.E., Lomas, A., Morgan, A., Humphries, J., Shuttleworth, C.A., and Kielty, C.M. (2003) Cell Adhesion to Fibrillin-1 Molecules and Microfibrils Is Mediated by $\alpha_5\beta_1$ and $\alpha_v\beta_3$ Integrins. *J. Biol. Chem.* **278**, 34605-34616

30. Jovanovic, J., Takagi, J., Choulier, L., Abrescia, N.G.A., Stuart, D.I., van Der Merwe, P.A., Mardon, H.J., and Handford, P.A. (2007) αvβ6 is a novel receptor for human fibrillin-1. Comparative studies of molecular determinants underlying integrin-RGD affinity and specificity. *J. Biol. Chem.* **283**, 6743-6751

31. Hass, T.A., and Plow, E.F. (1994) Integrin-ligand interactions: a year in review. *Current Opinion in Cell Biol.* **6**, 656-662

32. Ruoslahti, E. (1996) RGD and other recognition sequences for integrins. *Annu. Rev. Cell Dev. Biol.* **12**,697-715

33. Campbell, I.D., and Humphries, M.J. (2011) Integrin structure, activation and interactions. *Cold Spring Harb Perspect Biol.* **1**, 3(3)

34. Humphries, J.D., Byron, A., and Humphries, M.J. (2006) Integrin ligands at a glance. *J Cell Sci.* **1;**119

35. Lee, S.S.J., Knott, V., Jovanovic, J., Harlos, K., Grimes, J.M., Choulier, L., Mardon, H.J., Stuart, D.I., and Handford, P.A. (2004) Structure of the Integrin Binding Fragment from Fibrillin-1 Gives New Insights into Microfibril Organization. *Structure.* **12**, 717-729

36. Hynes, R.O. (2002) Integrins: bidirectional, allosteric signaling machines. *Cell.* **110**, 673-687

37. Wagner, C.L., Mascelli, M.A., Neblock, D.S., Weisman, H.F., Coller, B.S., and Jordan, R.E. (1996) Analysis of GPIIb/IIIa receptor number by quantification of 7E3 binding to human platelets. *Blood.* **88**, 907-914

38. Richardson, J.S. (1981) The Anatomy & Taxonomy of Protein Structure. *Adv. Prot. Chem.* **34**, 167-339

39. Hansen, R., E., Ostergarrd, H., Norgaard, P., and Winther, J.R. (2007) Quantification of protein thiols and dithiols in the picomolar range using sodium borohydride and 4,4'-dithiodipyridine. *Analytical Biochemistry*. **363**, 77-82

40. Schilling, S.H., Hjelmeland, A.B., Rich, J.N., and Wang, X. (2008) TGF-β: A multipotential cytokine. *Cold Spring Harb Laboratory Press.* **1**, 45-77

41. Roberts, A.B., and Sporn, M.B. (1996) Transforming growth factor-β. In the molecular and cellular biology of wound repair. (ed. R.A.F.), pp. 419-472. Plenum Press, New York.

42. Abe, M., Harpel, J.G., Metz, C.N., Nunes, I., Loskutoff, D.J., and Rifkin, D.B. (1994) An assay for transforming growth factor-β using cells transfected with a plasminogen activator inhibitor-1 promoter-luciferase construct. *Analytical Biochem.* **216**, 276-284

43. Dickinson, C.D., Veerapandian, B., Dai, X.P., Hamlin, R.C., Xuong, N., Ruoslahti, E., and Ely, K.R. (1994) Crystal Structure of the Tenth Type Ill Cell Adhesion Module of Human Fibronectin. *J. Biol. Chem.* **236**, 1079-1092

44. Krerel, A.M., Wagner, C., Seymour-Ulmer, J., and Lazarus, R.A. (1994) Structure of the RGD Protein Decorsin: Conserved Motif and Distinct Function in leech Proteins that Affect Blood Clotting. *Science* **264**, 1944-l 947

45. Koivunen, E., Wang, B., and Ruoslahti, E. **(**1994) Isolation of a highly specific ligand for the $\alpha_5\beta_1$ integrin from a phage display library. *J. Cell Biol.* **124**, 373–80

46. Cheng, S., Craig, W.S., Mullen, D., Tschopp, J.F., Dixon, D., and Pierschbacher, M.D. (1994) Design and synthesis of novel cyclic RGD-containing peptides as highly potent and selective integrin $\alpha_{IIb}\beta_3$ antagonists. *J. Med. Chem.* **37**, 1–8

47. Aota., S., Nomizu, M., and Yamada, K.M. (1994) The short amino acid sequence Pro-His-Ser-Arg-Asn in human fibronectin enhances cell-adhesive function. *J. Biol. Chem.* **269**, 24756-24761

48. Mould, A.P., Askari, J.A., Aota, S., Yamada, K.M., Irie, A., Takada, Y., Mardon, H.J., and Humphries, M.J. (1997) Defining the topology of integrin α5β1-fibronectin interactions using

inhibitory anti-αv and anti-β1 monoclonal antibodies. Evidence that the synergy sequence of fibronectin is recognized by the amino-terminal repeats of the alpha5 subunit. *J. Biol. Chem.* **272**,17283-17292

49. Danen, E.H.J., Aota, S.I., Vankraats, A.A., Yamada, K.M., Ruiter, D.J., and Vanmuijen, G.N.P. (1995) Requirement for the Synergy Site for Cell-Adhesion to Fibronectin Depends on the Activation State of Integrin α5β1. *J Biol. Chem.* **270**, 21612-21618
50. Jovanovic J., Iqbal S., Jensen S., Mardon, H., and Handford, P. (2008) Fibrillin-integrin interactions in health and disease. *Biochem Soc Trans.* **36**, 257-262
51. Weinreb, P.H., Simon, K.J., Rayhorn, P., Yang, W.J., Leone, D.R., Dolinski, B.M., Pearse, B.R., Yokota, Y., Kawakatsu, H., Atakilit, A., Sheppard, D., and Violette, S.M. (2004) Function-blocking integrin αvβ6 monoclonal antibodies. Distinct ligand-mimetic and nonligand-mimetic classes. *J. Biol. Chem.* **279**, 17875-17887
52. Weinacker, A., Chen, A., Agrez, M., Cone, R.I., Nishimura, S., Wayner, E., Pytela, R., and Sheppard, D. (1993) Role of integrin αvβ6 in cell attachment to fibronectin. Heterologous expression of intact and secreted forms of the receptor. *J. Biol. Chem.* **269**, 6940-6948
53. Yokosaki, Y., Monis, H., Chen, J., and Sheppard, D. (1996) Differential effects of the integrins α9β1, αvβ3 and αvβ6 on cell proliferative responsive to tenascin. Roles of the β subunit extracellular and cytoplasmic domains. *J. Biol. Chem.* **271**, 24-44-24150
54. Schnapp, L.M., Hatch, N., Ramos, D.M., Klimanskaya, I.V., Sheppard, D., and Pytela, R. (1995) The human integrin α8β1 functions as a receptor for tenascin, fibronectin, and vitronectin. *J. Biol. Chem.* **270**, 23196-23202
55. Jackson, T., Clark, S., Berryman, S., Burman, A., Cambier, S., Mu, D., Nishimura, S., and King, A.M.Q. (2004) Integrin αvβ8 functions as a receptor for foot-and-mouth disease virus: Role of the β-chain cytodomain in integrin-mediated infection. *J. Virol.* **78**, 4533-4540

**Publishing Agreement**

*It is the policy of the University to encourage the distribution of all theses, dissertations, and manuscripts. Copies of all UCSF theses, dissertations, and manuscripts will be routed to the library via the Graduate Division. The library will make all theses, dissertations, and manuscripts accessible to the public and will preserve these to the best of their abilities, in perpetuity.*

***Please sign the following statement:***

*I hereby grant permission to the Graduate Division of the University of California, San Francisco to release copies of my thesis, dissertation, or manuscript to the Campus Library to provide access and preservation, in whole or in part, in perpetuity.*

Author Signature

9-5-2018
Date